NTNU

Norwegian University of
Science and Technology

Development of the Pressure-Time as a Relative Method

Helene Njølstad Dagsvik

Master of Energy and Environmental Engineering
Submission date: January 2017
Supervisor: Michel Jose Cervantes, EPT

Norwegian University of Science and Technology
Department of Energy and Process Engineering

NTNU

Norwegian University
of Science and Technology

Department of Energy
and Process Engineering

EPT-M-2016-179

MASTER THESIS

for

Student
Helene Njølstad Dagsvik

Autumn 2016

Development of the pressure-time as a relative method

Utvikling av trykk-tid som en relativ metode

Background and objective

The efficiency of hydraulic turbines is an essential parameter to power plant owners. This parameter is measured every 10 years to check eventual deviation. In low head machines, the determination of the flow rate is usually performed with the Winter-Kennedy method. This method is relative and has shown some inconsistencies o er time. An alternative method is thus desirable. The alternative method should be simple and have a similar cost to the Winter-Kennedy method. The pressure-time method may be an alternative.
The pressure-time method is an absolute method allowing the determination of the flow rate with a good accuracy under specific conditions, see IEC 41 standard. The method is based on the measurements of the differential pressure between 2 cross-sections in the penstock during a closure of the guide vanes. A major condition to perform accurate measurements is a straight pipe of constant cross-section
In the present project, the pressure time method will be evaluated as a relative method. Measurements previously performed at the Water Laboratory will be used for this purpose.

The following tasks are to be considered:

1 Literature review
2 Develop a code to determine the relative flow rate using the pressure-time method
3 Evaluate relative pressure-time measurements performed on a test rig at NTNU
4 Develop a numerical model using the method of characteristics (MOC) to simulate the experimental measurements previously performed
5 Determine the limitation and potential of the method with application to hydraulic turbines

Within 14 days of receiving the written text on the master thesis, the candidate shall submit a research plan for his project to the department.

When the thesis is evaluated, emphasis is put on processing of the results, and that they are presented in tabular and/or graphic form in a clear manner, and that they are analyzed carefully.

The thesis should be formulated as a research report with summary both in English and Norwegian, conclusion, literature references, table of contents etc. During the preparation of the text, the candidate should make an effort to produce a well-structured and easily readable report. In order to ease the evaluation of the thesis, it is important that the cross-references are correct. In the making of the report, strong emphasis should be placed on both a thorough discussion of the results and an orderly presentation.

The candidate is requested to initiate and keep close contact with his/her academic supervisor(s) throughout the working period. The candidate must follow the rules and regulations of NTNU as well as passive directions given by the Department of Energy and Process Engineering.

Risk assessment of the candidate's work shall be carried out according to the department's procedures. The risk assessment must be documented and included as part of the final report. Events related to the candidate's work adversely affecting the health, safety or security, must be documented and included as part of the final report. If the documentation on risk assessment represents a large number of pages, the full version is to be submitted electronically to the supervisor and an excerpt is included in the report.

Pursuant to "Regulations concerning the supplementary provisions to the technology study program/Master of Science" at NTNU §20, the Department reserves the permission to utilize all the results and data for teaching and research purposes as well as in future publications.

The final report is to be submitted digitally in DAIM. An executive summary of the thesis including title, student's name, supervisor's name, year, department name, and NTNU's logo and name, shall be submitted to the department as a separate pdf file. Based on an agreement with the supervisor, the final report and other material and documents may be given to the supervisor in digital format.

☐ Work to be done in lab (Water power lab, Fluids engineering lab, Thermal engineering lab)
☐ Field work

Department of Energy and Process Engineering, 22. August 2016

Olav Bolland
Department Head

Michel Cervantes
Academic Supervisor

Research Advisor: Torbjørn Nielsen

Preface

This thesis was written in the Waterpower Laboratory at NTNU during the fall of 2016. The main objective of my work has been to perform an experimental and numerical examination of the relative pressure-time method using laboratory measurements.

I would like to thank my supervisor, Michel Cervantes, for his availability, guidance and knowledge. Not to forget for his patience with me and for not giving me up despite my (sometimes hopeless) misunderstandings and considerations. I hope my struggles have paid off and that my work may be of use in the future.

I would also like to give a special thanks to Tore, who has been caring for me, encouraged me and endured with my unpredictable mood the last 21 weeks. I promise that I will do tons of housecleaning in the times to come.

Helene Njølstad Dagsvik
January 23, 2017
Trondheim

Abstract

Hydropower has played an essential role in the Norwegian power production over the last century. Approximately $99.9\ \%$ of the total production comes from renewable sources, of which hydropower represent $99\ \%$. Changes in runner materials and designs have contributed to a tremendous improvement of the overall turbine efficiency. Several methods of calculating the efficiency exists today, aiming to determine the performance of various turbines under various circumstances. Efficiency measurements in low-head machines have proven to be challenging, as difficult pipe geometry and short water inlets complicate the use of traditional measuring techniques.

The object of this thesis has been to evaluate the pressure-time method as a relative method and examine the method's potential for application in hydraulic machines. Experimental pressure-time measurements were performed at the Waterpower laboratory at NTNU during the spring of 2016. Two flows at approximately 170 and 400 l/s were repeatedly measured and evaluated based on the work by former Ph.D. student P. Jonsson from LTU in Sweden. The relative pressure-time method presented in this thesis has been developed based on the experimental laboratory measurements.

The pressure section used in the laboratory experiments was extended from 4 m to cover the entire area from the open reservoir to a pressure sensor 10 m upstream a closure valve. The geometrical constant was calculated using the laboratory pipe dimensions and incorporated into a developed MATLAB for further calculation of the relative pressure-time flow. Moreover, two numerical MOC codes were developed to verify the experimental results. One represents a simple pipeline with a maximum discharge of 400 l/s, while the second is a complex pipeline with a discharge of 600 l/s.

The relative measurements show good accordance with the electromagnetic flowmeter installed on the test rig. Maximum discharge errors of $3.38\ \%$ and $2.56\ \%$ were found for the flows at 170 and 400 l/s, respectively. The numerical testing gave promising results with discharge errors of $0.15\ \%$ and $0.47\ \%$ for the simple and the complex pipeline.

Low random errors over a wide range of repetitions implies consistency between the relative measurements. Moreover, an approach of the pipe factor provided final flows close to the reference flows recorded by the electromagnetic flowmeter. Evaluation of the presented method suggests that a relative pressure-time approach may possibly be relevant for future low-head machine testing.

Sammendrag

Vannkraft har spilt en viktig rolle i Norsk energiproduksjon gjennom det siste århundet. Fornybare energikilder står for omtrent $99{,}9\ \%$ av den totale produksjonen, hvorav vannkraft alene utgjør hele $99\ \%$. Endringer i løpehjulsmaterialer og design har bidratt til en enorm forbering av den totale turbinvirkningsgraden. Flere forskjellige metoder eksisterer i dag for å beregne virkningsgraden til ulike typer turbiner under ulike omstendigheter. Virkningsgradsmålinger av lavtrykksturbiner har vist seg å være utfordrende, da vanskelige rørgeometrier og korte vannveier ofte er tilstede og kompliserer bruken av tradisjonelle måleteknikker.

Målet med denne masteroppgaven har vært å evaluere trykk-tid-metoden som en relativ metode og å undersøke metodens potensial for videre bruk i hydrauliske maskiner. Trykk-tid målinger ble gjennomført i Vannkraftlaboratoriet ved NTNU våren 2016. To vannføringer ved omtrent 170 og 400 l/s ble gjentatte ganger målt og evaluert basert på arbeidet til tidligere Ph.D. student P. Jonsson fra LTU i Sverige. Den relative trykk-tid-metoden presentert i denne masteroppgaven har blitt uviklet ved hjelp av de eksperimentelle laboratoriemålingene.

Trykkseseksjonen som ble benyttet i laboratorieeksperimentene ble utvidet fra 4 m til å omfatte hele området fra reservoiret til en trykksensor 10 m oppstrøms en lukkeventil. Den geometriske konstanten ble beregnet for den nye rørgeometrien og inkludert i en MATLAB-kode utvilket for videre beregninger av den relative trykk-tid vannføringen. To numeriske MOC-koder ble også utviklet for å verifisere de eksperimentelle resultatene. Den første koden representerer en enkel rørstrekning med en maksimal vannføring lik 400 l/s. Den andre representerer en kompleks rørstrekning med en vannføring lik 600 l/s.

De relative målingene viser et godt samsvar med det elektromagnetiske flowmeteret montert på testriggen. Det ble funnet maksimale vannføringsfeil på henholdsvis $3.38\ \%$ og $2.56\ \%$ for vannføringene på 170 of 400 l/s. De numeriske testene ga lovende resultater med vannføringsfeil på henholdvis $0.15\ \%$ og $0.47\ \%$ for den enkle og den komplekse rørstrekningen.

Tilfellet av små, tilfeldige feil over et stort spekter av repetisjoner tilsier god samsvarhet mellom de relative målingene. En tilnærming av rørfaktoren gir dessuten også vannføringer nær referansestrømmen registrert av det elektromagnetiske flowmeteret. Den presenterte metoden antyder at en relativ tilnærming til trykk-tid metoden kan være relevant for fremdige målinger i lavtrykksmaskiner.

Table of Contents

List of Figures

List of Tables

Abbreviations

NTNU	The Norwegian University of Science and Technology
LTU	Luleå University of Technology
MOC	Method of Characteristics
IEC	The International Electrotechnical Commission
RSS	Root of the Sum of the Squares
PDE	Partial Differential Equation
ODE	Ordinary Differential Equation
DAQ	Data Acquisition
BEP	Best Efficiency Point
Eq.	Equation

Nomenclature

Symbol:	Description:	Unit:
Q_{rel}	Relative discharge	$[\%]$
Q_i	Relative discharge	$[m^3/s]$
$Q_{i\,ref}$	Reference discharge	$[m^3/s]$
f_t	Overall error	$-$
f_s	Systematic uncertainty	$-$
f_r	Random uncertainty	$-$
X_i	Observation number i	$-$
$\bar{X}$	Arithmetic mean of X	$-$
X_{ref}	Reference measurement	$-$
n	Number of observations	$-$
S_X	Estimated standard deviation	$-$
v	Degree of freedom	$-$
e	Discharge error	$[\%]$
e_r	Random error	$[\%]$
L	Length of measuring section	$[m]$
A	Cross-sectional area of pipe section	$[m^2]$
D	Diameter of pipe	$[m]$
V	Velocity of fluid	$[m/s]$
t	Duration of measurements	$[s]$
t_0	First integration point	$[s]$
t_1	Last integration point	$[s]$
t_c	Duration of closure	$[s]$
Q	Discharge	$[m^3/s]$
Q_0	Initial discharge	$[m^3/s]$
ΔQ	Discharge segment	$[m^3/s]$
q	Leakage water	$[m^3/s]$
ΔP	Differential pressure	$[Pa]$
ΔP_s	Differential static pressure	$[Pa]$
ΔP_d	Differential dynamic pressure	$[Pa]$
P_1	Pressure section 1	$[Pa]$
P_2	Pressure section 2	$[Pa]$
P_{atm}	Atmospheric pressure	$[Pa]$
z	Elevation above reference	$[m]$
g	Gravitational acceleration	$[m/s^2]$
x	Length in axial direction of pipe	$[m]$
F	Pipe factor	$-$

$\Delta P_{L,f}$	Frictional pressure losses	$[Pa]$
$\Delta P_{L,m}$	Minor pressure losses	$[Pa]$
f	Darcy friction factor	$[-]$
f_q	Quasi-steady friction	$[-]$
Re	Reynolds number	$[-]$
K_L	Minor loss coefficient	$[-]$
k_1	Geometrical constant	$-$
k_2	Pressure loss constant	$-$
a	Wave speed	$[m/s]$
k	Brunone friction coefficient	$[-]$
C^*	Vardy shear decay coefficient	$[-]$
K	Bulk modulus of elasticity of fluid	$[Pa]$
E	Young modulus	$[Pa]$
e	Thickness of pipe	$[m]$
H	Piezometric head	$[m]$
C^+	Positive characteristic line	$-$
C^-	Negative characteristic line	$-$
Δx	Length of pipe section	$[m]$
Δt	Time step	$[s]$
N	Number of nodes	$-$
HR	Head of upper reservoir	$[m]$
HR_2	Head of lower reservoir	$[m]$
HP	Head one time step ahead	$[m]$
QP	Discharge one time step ahead	$[m^3/s]$
K_v	Valve loss coefficient	$[-]$
c_d	Flow coefficient	$[-]$

Greek symbols

Symbol:	**Description:**	**Unit:**
ρ	Density of water	$[kg/m^3]$
ξ	Pressure losses	$[Pa]$
ξ_0	Initial pressure losses	$[Pa]$
α	Coriolis correction factor	$[-]$
ε	Pipe roughness	$[-]$

1 Introduction

Hydraulic efficiency tests are performed to reveal important information regarding the state of a hydraulic turbomachine. It is a necessary tool to ensure that the efficiency warranties of a contract are met when installing a new turbine or pump. Efficiency tests are also highly useful when investigating the improvement of a turbine before and after a refurbishment, and for operational planning in a cost-effective perspective. Moreover, regularly efficiency measurements of a turbine reveal the progress of wear through years of operation and may give an indication of the remaining lifetime of a machine. It is not unusual for modern turbines to have efficiencies above 90 %. Large Francis turbines operating at best efficiency point (BEP) at medium heads may achieve efficiencies close to 94 – 96 % (Brekke, 2001). The terms and conditions of performing field acceptance tests on hydraulic turbomachines are stated in the IEC 41 standard (IEC 41, 1991a).

There are several different methods of determining the efficiency of a turbine. The choice of method depends on the available pressure head and discharge, costs associated with the measuring equipment and implementation, design and geometry of the hydropower plant and operative conditions. Some of the most common methods used today include the thermodynamic, ultrasound, pressure-time (Gibson), current-meter and the Winter-Kennedy method. Most of the methods aim to determine the flow rate in the pipeline for an indirectly approach of the efficiency. One exception is the thermodynamic method, which determines the efficiency by utilizing the temperature increase through the turbine by assuming that the entire energy loss has been converted into heat.

Hydropower plants are classified by their gross head. Low-head plants are designated in the range 2 – 30 m, medium-head plants are in the range 30 – 250 m and high-head plants are classified as heads greater than 250 m (Subramanya, 2013). Choice of efficiency method strongly depends on the available head, as the obtainable efficiencies varies according to the operating conditions present. The uncertainties that are expected to be found by following the recommended terms for various methods are shown in Figure 1-1:

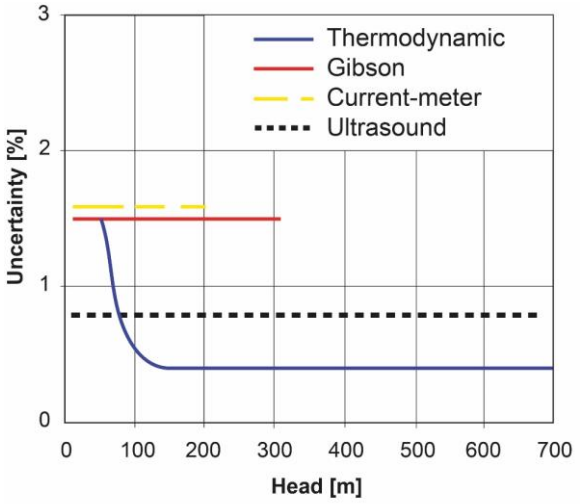

Figure 1-1: Variation in uncertainties as a function of available heads (Nielsen, 2015).

The thermodynamic method is clearly best suited for high-head machines, as the uncertainty decreases with increasing head. The operating ranges of the current-meter and Gibson are limited to low-head and medium-head machines, while the ultrasound method succeeds to provide somewhat constant uncertainties for a wide range of heads.

In Norway, the hydroelectric power production covers 99 % of the total power production. The thermodynamic method is widely used, due to the large number of high mountains and consequently many high-head plants. Several low-head machines are installed in Norwegian rivers, and the incidence of small hydropower plants have increased recent years due to the arrangement of governmental subsidies in terms of green certificates. The varying amount of power plants demands knowledge about various efficiency methods to unveil the true performance of the power production.

The hydraulic efficiency methods are classified either as absolute or relative. Relative measurements, commonly referred to as index tests, are usually performed to monitor the decrease in efficiency over time and to investigate the improvement after refurbishment. Any method may be used as a relative method, but the Winter-Kennedy is essentially preferred. The discharge measurements shall, according to the IEC 41 (1991) standard, be entirely absolute. However, the standard encourages use of relative tests for either comparison with absolute methods or as an alternative when absolute measurements are difficult to perform. It is often a challenging task to perform precise efficiency measurements when dealing with low-head machines. Challenging geometrical variations in the pipeline and short inlet passages are often present in low-head power plants. In such cases, a cost effective and simple alternative method is requested, typically the Winter-Kennedy. The procedure of executing the Winter-Kennedy method is presented in the IEC 41 (1991) standard and includes recording of the pressure at the inner and outer wall in a cross section of the spiral casing. This provides a calculation of the volume flow rate by the relation $Q =$

$k \cdot \Delta h^n$, where *k* is a calibrated constant, *n* is a number between 0.48 and 0.52 and Δh is the differential pressure. Although the Winter-Kennedy method is quite frequently preferred in low-head machines, it has shown some inconsistency over time. It is especially sensitive for modifications in the pipeline, which may cause a slight change in the flow pattern and affect the relative measurements. Problems caused by the inlet boundary layer was examined experimentally by J. Nicolle and G. Proulx (Nicolle and Proulx, 2010), who found deviations in the inflow condition of 5.4 %. Winter-Kennedy model testing done to examine the effects of skew inlet flow (Andersson et al., 2008), provided deviations close to 10 %. However, the method has given errors as low as 1 % under favorable conditions, but variations over time appear to be the pervasive problem. In need of an accurate, consistent alternative, the relative pressure-time method has been suggested as an option. P. Jonsson performed a relative analysis on Porjus U9 and presented the possibility of achieving accurate results using a relative pressure-time approach (Jonsson and Cervantes, 2013).

A relative measurement is found by indexing the experimental flow rate against a reference flow, and is in the IEC 41 (1991) defined as:

$$Q_{rel} = \frac{Q_i}{Q_{ref}} \qquad (1.1)$$

where Q_{rel} denotes the percentage size of the relative measurement, Q_i is the discharge measured during the testing and Q_{ref} denotes the value of the reference flow. The value of the reference flow may be represented in terms of previous, absolute measurements or by the guarantees from the contractors. A third option is to use the best relative flow achieved in the measurements as the reference, assuming a probable absolute flow.

Both random and systematic errors must be considered in the evaluation of absolute measurements. Errors associated with relative tests, on the other hand, are entirely random, implying that systematic errors are entirely neglected in the statistical analysis. However, a series of repetitions are required in order to evaluate the random errors thoroughly.

1.1 Objective of thesis

The main objective of this thesis is to evaluate the pressure-time method as a relative method. To this purpose, data from previously pressure-time measurements performed in the Waterpower Laboratory at NTNU will be evaluated. The Gibson test rig located in the laboratory allows for controlled measurements outside the IEC 41 (1991) standard and is suited for a relative evaluation of the pressure-time method. The relative analysis will elaborate the concerns regarding complex geometry and unknown losses in the test rig. A further investigation of the repeatability and assessment of the uncertainties is also

presented for a thorough evaluation of the method. Furthermore, a numerical model is developed to support the experimental findings.

1.2 Structure of thesis

The first part of the thesis introduces the pressure-time method and presents limitations and advantages associated with carrying out the measurements. A literature study covers recent progress of the method and discusses the problems associated with the hydraulic losses. An introduction to the numerical modelling is further presented, followed by a representation of the experimental test case setup and the modelling procedure. Furthermore, the experimental and numerical results are presented and evaluated, followed by a discussion of the method's validity and further application in low-head machines. This master is a continuation of the project work written during the spring of 2016 (Dahl, 2016).

1.3 Evaluation of uncertainties

In statistical analysis, an error states how much a measurement deviates from its true value. The uncertainties of a measurement form an interval where the true value is very likely to lie within. A confidence interval of 95 % is commonly used, implying that it is likely that 95 % of the interval estimates include the true value.

Three different types of errors must be considered in a statistical analysis, known as spurious errors, systematic errors and random errors:

1. **Spurious errors:**
   Spurious errors are caused by human or instrumental failure. They usually occur as outliers and must be removed for further statistical analysis.

2. **Systematic errors:**
   Systematic errors are caused by equipment errors, calibration flaws and improper use of instruments and are not directly related to the actual measurements. Systematic errors cannot be reduced by repeating the measurements and may be difficult to estimate. The guaranteed systematic error of a given equipment is usually specified by the manufacturer, but some equipment require additional calibration to reveal the actual uncertainties.

3. **Random errors:**
   Random errors are caused by unknown and unpredictable changes in the measurements and are due to variations in the system or by instability in the measuring equipment. They may for instance occur by changes in the water temperature or by noises in the electrical installation. These errors are reduced by increasing the number of repetitions.

The overall uncertainty f_t of a measurement is achieved by combining the systematic and random uncertainties by the root of the sum of the squares method (RSS). This assumes that the systematic and random errors are independent of each other:

$$f_t \pm (f_s^2 + f_r^2)^{1/2} \qquad (1.3.1)$$

where f_s and f_r denote the systematic and relative uncertainties, respectively.

1.3.1 Random uncertainties

The random uncertainties for repetitive measurements under constant operational conditions are estimated by following the instructions stated in *Appendix D* in the IEC 41 (IEC 41, 1991b) standard.

For a given number of observations $X_1, X_{2,\dots,} X_n$, the arithmetic mean $\bar{X}$ is found by:

$$\bar{X} = \frac{1}{n}\sum_{i=1}^{n} X_i \qquad (1.2.2)$$

where X_i is the value of the i^{th} measurement of X and n is the total number of measurements.

The standard deviation σ describes the spread of a data set and indicates how far a single measurement deviates from the mean. For a limited amount of measurements, only an estimation of the standard deviation is obtainable. The estimated standard deviation s_X is given by:

$$s_X = \left(\frac{1}{n-1} \sum_{i=1}^{n} [X_i - \bar{X}]^2 \right)^{1/2} \qquad (1.3.3)$$

IEC 41 (1991) requires that the random uncertainties lie within a 95 % confidence interval, corresponding to 1.96 standard deviations. For an estimated standard deviation, the criterion is met using the Student's t distribution. For n measurements, the degree of freedom is defined as $v = n - 1$. The corresponding $t's$ from the Student's distribution are found in Table 1-1:

Degrees of freedom $v = n - 1$	**Student's** t For the 95 % confidence level	$t/\sqrt{n}$
1	12.706	8.984
2	4.303	2.484
3	3.182	1.591
4	2.776	1.241
5	2.571	1.050
6	2.447	0.925
7	2.365	0.836
8	2.306	0.769
9	2.262	0.715
10	2.228	0.672
11	2.201	0.635
12	2.179	0.604
13	2.160	0.577
14	2.145	0.554
15	2.131	0.533
20	2.086	0.455
30	2.042	0.367
60	2.000	0.256
∞	1.960	0

Table 1-1: Values of the Student's t distribution (IEC 41, 1991c)

The random uncertainty of the measurements at a 95 % confidence interval is further achieved by the following relation:

$$f_r = \pm \frac{t\, s_X}{\sqrt{n}} \qquad (1.3.4)$$

Then the true value of a measurement is likely to be found a distance f_r from the mean value $\overline{X}$:

$$\bar{X} \pm f_r \qquad (1.3.5)$$

with a corresponding percentage error equal:

$$e_r = \frac{f_r}{\bar{X}} \cdot 100 \qquad (1.3.6)$$

1.3.2 Reference comparison

The overall error e is found when comparing an experimental measurement X_i to a reference measurement X_{ref} by

$$e = \frac{X_i - X_{ref}}{X_{ref}} \cdot 100 \qquad (1.3.7)$$

2 The pressure-time method

The pressure-time method, also known as the Gibson method, was introduced by Norman Gibson in 1923 (Gibson, 1923). The method involves measuring the arising retardation pressure between two measuring sections while closing the guide vanes, needles or valve upstream a turbomachine in a closed conduit. By integrating the differential pressure as a function of the sampling time, the total discharge in the pipeline can be calculated for further evaluation of the turbine efficiency.

Over the recent years the method has been greatly improved due to development of more precise measuring equipment, improved data processing and more accurate instrumental calibration. According to the IEC 41 (1991), the method can, favorable conditions, estimate the flow rate in the pipeline with an overall uncertainty of 1.5 – 2 % at the 95 % confidence level.

There are several advantages associated with the pressure-time method. The method does not require much equipment compared to similar options and is therefore a rather cheap alternative. Several power plants have preinstalled pressure taps on the inlet pipe to the turbomachine, which entails efficient and simple installation of the pressure equipment. Moreover, the method requires little downtime, which is preferable in a cost-effective perspective.

There are, however, several difficulties and limitations associated with application of the pressure-time method, stated in the IEC 41 (1991) standard. The distance between the two measuring sections must be a straight pipe section with a length of at least 10 m and a constant cross-sectional area. This is rarely the case in small, low-head power plants, due to the incidence of variations in the pipe geometry and short water inlets. Additionally, the product of the pipe length and the mean velocity of the water (VL) should be at least $50\ m^2/s^2$. One of the main challenges concerns the determination of the final flow. It is difficult to determine the final integration point, due to the arising pressure oscillations after complete shut-off. A large variation in the final flow may be found by variation of the final integration point, and the cut-off time must therefore be evaluated carefully. Despite strict demands and limitations regarding the application of the method, the possibility of using the method for complex pipes has not excluded from the standard.

2.1 The principles behind the pressure-time method

2.1.1 Newton second law

The pressure-time method is based on the principles behind Newton's second law and the fluid mechanical laws. When closing the guide vanes, a large differential pressure between the two measuring sections occurs due to a change in momentum. This gives a relation between the rise in pressure and the deceleration of mass:

$$\rho L A \frac{dV}{dt} = -A\Delta P \qquad (2.1.1)$$

The setup of the pressure-time procedure is illustrated in Figure 2-1:

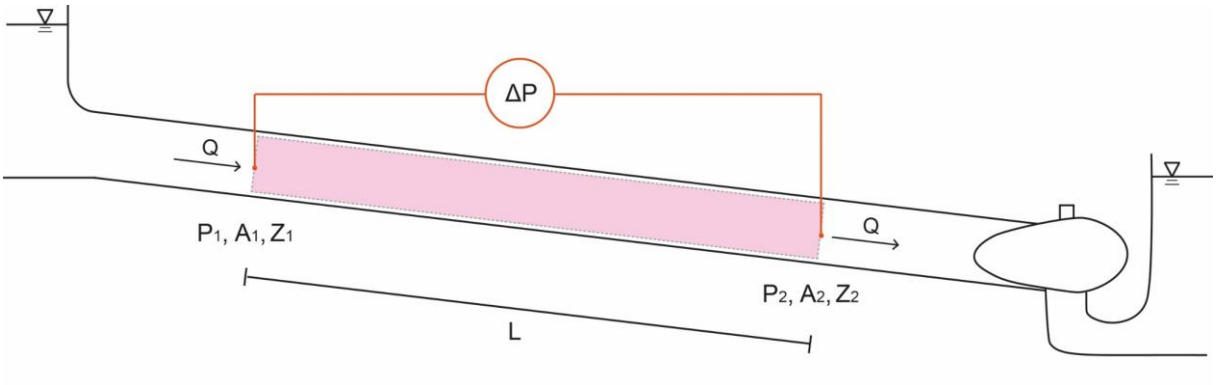

Figure 2-1: Setup of pressure-time measurements

During the closure, a pressure wave forms upstream the closure device and propagates at high speed back and forth throughout the entire pipeline. The closure time must be chosen to avoid the effects of these pressure waves, known as water hammers. If the closure is too rapid, the travelling wave may cause fatale damages, like rupture or collapse of the pipe.

The differential pressure $\Delta P = P_2 - P_1$ that is measured between pressure section 1 and 2 upstream the guide vanes, is illustrated as a function of time in Figure 2-2. The differential pressure, represented by the blue curve, increases during the closure until the closing device is completely shut-off at the time t_c. Pressure oscillations arise immediately after closure and fade out after some time.

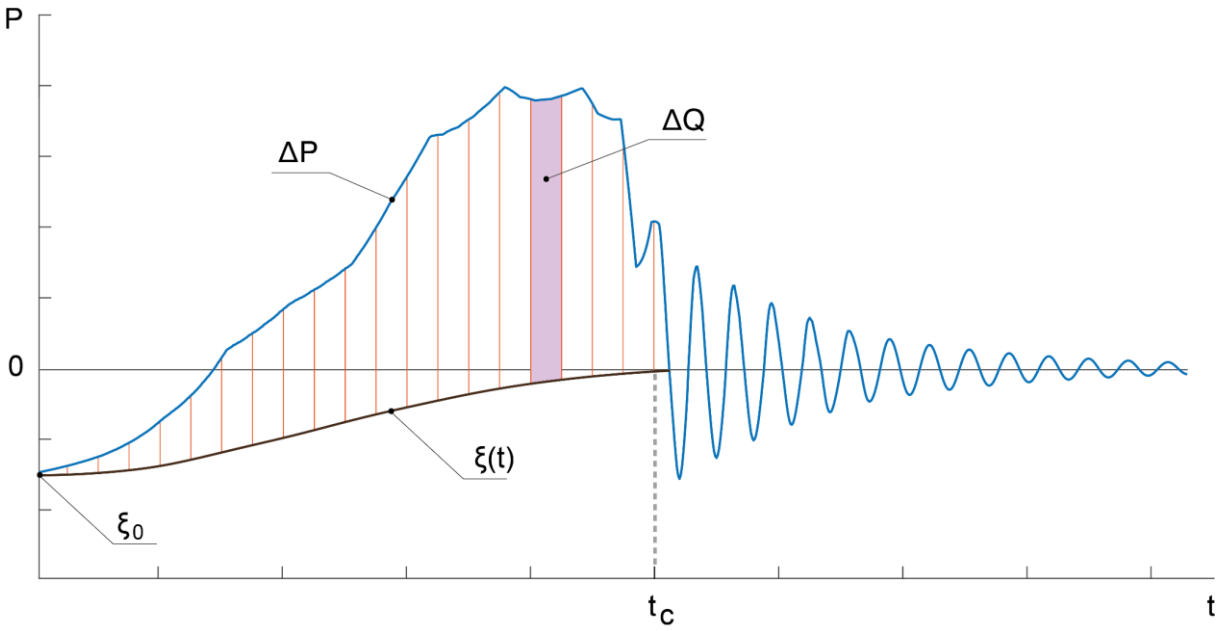

Figure 2-2: Pressure variaton during a closure

The initial flow may then be calculated using the pressure-time method by integrating the differential pressure as a function of the closure time. The pink shaded area specifies one flow segment ΔQ_i and is the area of the differential pressure over one time step. The final flow is found by summation of all flow segments. The number of flow segments are determined by the sample frequency, which should be at least 50 readings per second, as stipulated in the IEC 41 (1991).

The hydraulic pressure losses are denoted ξ and vary from the initial loss ξ_0 and throughout the closure. Between two sections in a straight pipeline, these losses are entirely frictional, due to the occurrence of shear stresses along the pipe wall. These losses must be subtracted from the differential pressure in the integration, as they constitute a noticeable impact of the overall differential pressure. It is essential to define the losses properly to avoid substantial errors in the final flow calculation.

The first integration point is chosen when the closing starts and the last integration point is chosen when the closing device is closed. It may be difficult to determine the last integration point due to the occurrence of pressure oscillations after closure and a mismatch between the shut-off of the closing device and the shut-off of the recorded flow. One procedure of determining the final integration point is thoroughly explained in the IEC 41 (1991). If the oscillations are small or fade out quickly, the final flow may be found by integrating over the pressure oscillations, as explained in (Jonsson, 2011). If the oscillations are small, but non-harmonic or noisy, the same procedure may still be carried out. However, due to varying fluctuations, an average over a range is required to achieve the finale flow.

2.1.2 Derivation of the pressure-time method

The pressure-time integral is derived from the general expression of the energy equation, which may be formulated as presented in (Adamkowski, 2012):

$$P_1 + \alpha_1 \frac{\rho Q^2}{2A_1^2} + \rho g z_1 = P_2 + \alpha_2 \frac{\rho Q^2}{2A_2^2} + \rho g z_2 + \xi + \rho \int_0^L \frac{dx}{A(x)} \frac{dQ}{dt} \qquad (2.1.2)$$

where P_1 and P_2 are the static pressures at section 1 and 2, respectively, ρ is the density of water, z_1 and z_2 are the elevations above a reference height, α_1 and α_2 are the Coriolis correction factors, L is the pipe length in the axial direction of x and $A(x)$ is the variation of the cross-sectional area as a function of x.

The geometrical pipe factor F depends on the pipe area, pipe length and fluid density and is in (Adamkowski, 2012) defined as

$$F = \rho \int_0^L \frac{dx}{A(x)} \qquad (2.1.3)$$

For a straight pipe with a constant cross-sectional area, Eq. (2.1.3) simplifies to

$$F = \rho \frac{L}{A} \qquad (2.1.4)$$

In Eq. (2.1.2), dQ/dt represents the unsteady flow, which equals zero under steady state conditions. By substituting Eq. (2.1.3) into Eq. (2.1.2), the energy equation may be rewritten to

$$\rho F \frac{dQ}{dt} = (P_1 + \rho g z_1 - P_2 - \rho g z_2) + \left(\alpha_1 \frac{\rho}{2A_1^2} - \alpha_2 \frac{\rho}{2A_2^2} \right) Q|Q| + \xi \qquad (2.1.5)$$

$$\frac{dQ}{dt} = \frac{1}{\rho F} (\Delta P_s + \Delta P_d + \xi) \qquad (2.1.6)$$

where ΔP_s and ΔP_d denote the static and dynamic pressures, respectively. Furthermore, an expression of Q is achieved by:

$$Q - q = \frac{1}{\rho F}\int_{t_0}^{t_1} (\Delta P_s(t) + \Delta P_d(t) + \xi(t))\, dt \qquad (2.1.7)$$

q represents the leakage water and must be calculated separately and added to the final flow. t_0 and t_1 denote the first and last integration points. The pressure-time integral is in general presented as:

$$Q = \frac{A}{\rho L}\int_{t_0}^{t_1} (\Delta P(t) + \xi(t))\, dt + q \qquad (2.1.8)$$

Both the differential pressure ΔP and the frictional losses ξ vary with time and must be considered at each time step.

2.2 Hydraulic losses

The pressure losses appearing in a fully developed, internal pipe flow are caused by frictional and minor losses. Frictional losses ΔP_f are present due to viscous forces along the wall and are calculated by the Darcy-Weisbach equation (Çengel and Cimbala, 2006):

$$\Delta P_f = f \frac{\rho L}{2D} \frac{Q^2}{A^2} \qquad (2.2.1)$$

where f is Darcy friction factor which strongly depends on the Reynolds number Re. For laminar flows (Re < 2300), the friction factor f in a circular pipe is found by:

$$f = \frac{64}{Re} \qquad (2.2.2)$$

For turbulent pipe flows (Re > 4000), the friction factor is estimated by the implicit Colebrook-White equation:

$$\frac{1}{\sqrt{f}} = -2.0 \log\left(\frac{\varepsilon/D}{3.7} + \frac{2.51}{Re\sqrt{f}}\right) \qquad (2.2.3)$$

where ε denotes the roughness of the pipe. Minor losses arise as the flow passes through bends, fittings, valves, elbows, enlargements and contractions. Irregularities in the pipeline causes a mixing and separation of the passing flow, which induces additional losses, which must be considered along with the frictional losses. They are usually small compared to the frictional losses, but must be considered in pipelines with complex geometries and pipe junctions. The minor losses ΔP_m are defined as:

$$\Delta P_m = K_L \frac{\rho}{2} \frac{Q^2}{A^2} \qquad (2.2.4)$$

where K_L is loss coefficient. Loss coefficients are experimental coefficients, which depend on the geometry and design of the power plant components.

The total hydraulic pressure losses ξ through a circular pipeline are found by summation of the total frictional losses and minor losses:

$$\xi = \frac{\rho}{2}\left(\sum_{i=1}\frac{f_i L_i}{D_i A_i^2} + \sum_{j=1}\frac{K_{L,j}}{A_j^2}\right)\cdot Q^2 \qquad (2.2.5)$$

ξ depends on the variation in the pipe geometries, friction factors and loss coefficients.

2.3 Literature review

Assessment of the discharge is one of the main issues when determining the performance of a turbomachine and the pressure-time method has proven to give good results, due to its limitations and strict requirements. The latest pressure-time procedure was published in the IEC41 standard in 1991, aiming to provide guidance for application of the method. Since then, the performance of measuring equipment has been greatly improved, although the investigation of the pressure-time method has been somewhat limited. Recent research has aimed to expand the method for low-head machine application and improved the procedure of finding the final integration point.

Pontus Jonsson investigated the usage of the pressure-time method outside the standard by performing pressure-time measurements in the Waterpower Laboratory at NTNU (Jonsson, 2011). The measurements were conducted between measuring sections of 3, 6 and 9 meters, corresponding to mean velocities of $V = 2.4, 4.4$ and $5.8\ m/s$. He found that the random error of the discharge increased with a decreasing measuring section. For the measuring section of 3 m, the uncertainties were found to be within $\pm 2\ \%$ when using differential pressure sensors, and $\pm 3\ \%$ when using absolute pressure sensors. Likewise, for the measuring section at 9 m, both differential and absolute sensors provided uncertainties within $\pm 1\ \%$. All uncertainties were found at a 95 % confidence level and the experimental results were validated numerically. As a result of his work, the upcoming update of the IEC 41 standard will decrease the required measuring section from $10\ m$ to $8\ m$, which corresponds to a decrease in the VL relation from $50\ m^2/s$ to $40\ m^2/s$ (Cervantes et al., 2012).

Improvements of the pressure-time method have also been done regarding the calculation procedure of the pressure integral. A. Adamkowski and W. Janicki (Adamkowski and Janicki, 2010) proposed an improved procedure of finding the final integration point, due to an error in the original procedure described in the IEC 41 (1991). The standard fails to ensure a zero-integral to remove the effects of the free oscillations, caused by an inadequate mathematical consideration.

2.3.1 Friction issue

A sufficient friction model is, as previously discussed, essential in the iteration process of finding the final flow. Determination of a precise loss model is challenging, and incorrectly considerations will influence the value of the calculated flow. The hydraulic losses may be described by assuming either constant friction losses or quasi-steady friction losses. The calculation procedure described in the IEC 41 (1991) calculates the hydraulic losses by assuming quasi-steady conditions.

By assuming that the hydraulic losses follow a constant friction approach, the friction factor f maintains constant throughout the integration procedure. The Reynolds number and friction factor are found from the steady-state flow conditions and are included in Eq. (2.2.1). An iterative solution of the pressure-time integral must be found, since the final flow rate Q in the pressure-time integral also is included in the pressure losses. Since the friction factor depends on the initial flow conditions, a new value must be found at each iteration step. The pressure-time integral assuming constant friction is given in Eq. (2.3.1):

$$Q = \frac{A}{\rho L}\int_{t_0}^{t_1}(\Delta p - f\frac{L}{D}\frac{\rho Q^2}{2A^2})\,dt + q \qquad (2.3.1)$$

This approach assumes frictional losses exclusively and utilizes the available pipe geometry to find an estimate of the losses. Previous work performed by P. Jonsson (Jonsson et al., 2012) has shown that a constant friction assumption does not describe the losses sufficiently and provides an underestimation or an overestimation of the flow, due to the presence of hydraulic transients.

A quasi-steady friction consideration, however, assumes that the losses are steady at each time step. The ASME International Code (ASME PTC 18-2011, 2011) states that the losses are *"assumed to follow a fully turbulent velocity-squared pressure law"*, meaning that the recovery line can be described in terms of:

$$\xi(\mathrm{t}) = -\frac{\xi_0}{Q_0|Q_0|}\cdot Q(t)|Q(t)| = k_2 \cdot Q(t)|Q(t)| \qquad (2.3.2)$$

where ξ_0 denotes the initial pressure loss and Q_0 is the initial flow rate. The initial conditions are constant properties and are represented in terms of the constant k_2 . Both frictional and minor losses are included in the quasi-steady friction approach, as shown in Eq. (2.2.5). The pressure-time integral may then be represented as:

$$Q = \frac{A}{\rho L}\int_{t_0}^{t_1}\Delta p + k_2\, Q(t)|Q(t)|\;dt + q \qquad (2.3.3)$$

An iterative process, similar to the constant friction approach, is required for the quasi-steady assumption. The initial pressure losses remains constant in Eq. (2.3.2), but the initial flow rate depends on the final flow calculation, implying that k_2 must be included in the iteration process. Neither the constant friction nor the quasi-steady approach give a complete description of the pressure losses, as the behavior of the hydraulic transients is difficult to predict.

2.4 Friction modelling

The behavior of the frictional effects is commonly examined and improved by numerical modelling. The use of one-dimensional numerical models, such as the method of characteristics (MOC), are widely used and have proven to provide fast and simple approximations of the losses. Unsteady friction effects are challenging to account for, as they are substantial and somewhat unpredictable. These effects are present as a consequence of decelerating the flow during a closure, causing a pressure rise and the occurrence of compressibility effects.

A friction model was introduced by B. Brunone (Brunone et al., 1991) to evaluate the unsteady friction behavior. The model aims to combine the contributions from the quasi-steady and unsteady frictions and has become popular, as it is easy to implement into a numerical model:

$$f = f_q + \frac{kD}{V|V|}\left(\frac{\partial V}{\partial t} - a\frac{\partial V}{\partial x}\right) \qquad (2.4.1)$$

where f_q denotes the quasi-steady friction factor, k is the Brunone friction coefficient, D is the internal diameter of the pipe, V the mean velocity of the flow and a is the wave speed. The quasi-steady friction corresponds to the Darcy friction factor at each time step. The terms $\partial V/\partial t$ and $\partial V/\partial x$ represents the temporal and convective accelerations, respectively. If the Mach number is sufficiently low, the wave speed a is greater than the velocity of the fluid. Under these circumstances, the convective acceleration term in Eq. (2.4.1) provides only a slight contribution to the friction and may be neglected.

The unsteady Brunone friction model was later modified by Vitkovský (Bergant et al., 2001) to ensure a correct sign of the convective acceleration:

$$f = f_q + \frac{kD}{V|V|}\left(\frac{\partial V}{\partial t} + a\ sign(V)\left|\frac{\partial V}{\partial x}\right|\right) \qquad (2.4.2)$$

The Brunone friction coefficient k is usually found by trial and error. The value of k may be changed locally, although a constant approach has proved to provide good results. Vardy and Brown introduced a method of calculating the Brunone friction coefficient k (Vardy and Brown, 1996). The friction coefficient is then expressed by considering the Vardy shear decay coefficient C^*:

$$k = \frac{\sqrt{C^*}}{2} \qquad (2.4.3)$$

The shear decay coefficient depends on Reynolds number and is found by

$$C^*: \begin{cases} 0.00476 & if\ Re < 2300 \\ \dfrac{7.41}{Re^{log(14.3/Re^{0.05})}} & if\ Re \geq 2300 \end{cases} \qquad (2.4.4)$$

The main issue behind explaining the pressure losses is due to the occurrence of transients. Jonsson et al. (2012) developed a numerical model that incorporated the unsteady friction to account for the unsteadiness of the flow. This was done by including the flow at each time step into a simplified version of the Brunone friction model. His model succeeded to correct both the overestimated and underestimated flow, and the discharge estimation error appeared to be reduced by 0.4 %. The results did also provide a good agreement between his numerical model and experimental work. Later, the unsteady friction model was experimentally validated by G. Dunca (Dunca et al., 2013).

A numerical pressure-time model that accounted for the compressibility of the liquid and the deformation of the pipe walls, was introduced by A. Adamkowski and W. Janicki (Adamkowski and Janicki, 2013) by assuming constant friction. Later, G. Dunca (Dunca et al., 2016) developed a similar numerical model by incorporating the unsteady Brunone friction model into the standard Gibson model and the Adamkowski model. She managed to obtain errors close to zero, with errors of 0.006 %, 0.003 % and 0.002 % for flows at $0.160\ m^3/s$, $0.300\ m^3/s$ and $0.400\ m^3/s$, respectively. A greater error was found using the steady models, emphasizing the importance of a well-defined unsteady friction model.

2.5 Relative pressure-time

Investigation of the pressure-time method as a relative method is of interest when attempting to expand the limitations of the absolute method. A proper development of the relative pressure-time procedure may provide a cheap and simple evaluation of the discharge for hydropower plant with low-head machines and complex geometry. Instead of limiting the measuring section to a straight pipe, the relative method utilizes the entire pipe length from the upper reservoir to a measuring section upstream the closure device. There are, however, several challenges associated with the computation of the relative Gibson flow. While application of the absolute method presupposes knowledge of the pipe geometry, the relative method must deal with a complex pipeline with varying cross-sectional areas, pipe junctions and bends. The main issues behind the relative pressure-time evaluation concern the examination of the unknown pipe factor and the hydraulic pressure losses in the complex pipeline.

The pipe factor equation, introduced in Eq. (2.1.3), takes into account the variations in a pipeline geometry caused by varying diameters, bends, inlets, contractions and expansions. The representation of the pipe factor is simplified by presenting it as a geometrical constant k_1:

$$k_1 = \frac{1}{\rho F} \qquad (2.5.1)$$

This constant must be found either by computation or by comparison with another efficiency method. The relative pressure losses are treated as the quasi-steady discussed in paragraph 2.3.1, which adds the unknown pressure loss constant k_2 to the problem. As previously discussed, the loss constant must be determined by the initial pressure loss and the steady-state discharge. The pressure-time integral presented in Eq. (2.3.3) may then be reformulated to contain both unknown constants, k_1 and k_2:

$$Q = k_1 \int_{t_0}^{t} \Delta p + k_2\, Q(t)|Q(t)|\, dt + q \qquad (2.5.2)$$

The assessment of the relative flow may prove to be a rather difficult task, as the loss constant k_2 depends on the initial flow conditions, which depends on the geometrical constant k_1. The first challenge is to compute a reasonable value of k_1. Moreover, an iterative model must be developed to compute iterative values of the loss constant and the final relative flow. The final challenge concerns the assessment of the developed method and its validity.

3 Numerical modelling

Hydraulic transients occur when steady state flows and pressures are transformed from a steady state condition to a time dependent state. Unsteady flow may be caused by opening or closing a valve, starting or stopping a pump, by variations in the reservoir level and by predictable and unpredictable operational changes. The appearance of hydraulic transients is unavoidable and must be controlled to avoid undesirable surges in the pipeline.

3.1 Water hammer

The water hammer phenomena, briefly discussed in paragraph 2.1.1, occurs in closed pipelines when the flow is decelerating rapidly due to a closure of a valve or guide vanes. The transients start immediately and transform the velocity of the flow into pressure, causing a rapid pressure rise upstream the closing device. This forms a water hammer, which propagates away from the device and through the entire system. The wave propagates back and forth until the wave is damped out due to friction and steady state is again achieved. If the valve is closed too rapidly, the water hammer may become too powerful and cause severe damages in the pipeline and pipe components. This is highly undesirable, and numerical modelling is usually performed to predict the pressure behavior when designing a new hydropower plant.

The velocity of the wave propagation, known as the wave speed, in a pipe with a circular cross-section is defined as:

$$a = \frac{\sqrt{K/\rho}}{\sqrt{1 + \left(\frac{K}{E}\right)\left(\frac{D}{e}\right)}} \qquad (3.1.1)$$

where a denotes the wave speed, K is the bulk modulus of elasticity of the fluid, ρ is the density, *E i*s the Young modulus of elasticity of the wall material, *D* is the diameter of the pipe and *e* is the thickness of the pipe. For rigid pipes with thick walls, the Young modulus goes towards infinity and the wave speed is simplified to $a \approx \sqrt{(K/\rho)}$. The wave speed depends on several factors and is a major source of uncertainty. Its value may vary due to the amount of air in the fluid, the pipe material and the condition of the pipeline (Lüdecke and Kothe, 2006). The modulus of elasticity is often difficult to determine and may contribute to the uncertainty as well. Moreover, the wave speed is affected by whether its positioned above the ground or buried.

The bulk modulus K represents the compressibility of the fluid. Water is usually considered incompressible, meaning that its density is assumed constant in a given system. This is usually a good approximation for water, presumed that the Mach number is low. However, the incidence of large pressure transients when closing a device causes rapid changes in pressure, and hence a consideration of the compressibility effects is necessary.

3.2 Transient modelling

The most frequently used mathematical method of modelling the water hammer phenomenon, is the method of characteristics, introduced by E. Wylie and V. Streeter (Wylie and Streeter, 1993). The method converts partial differential equations (PDEs) from the momentum and continuity equations into pure ordinary differential equations (ODEs), and allows for one-dimensional modelling of the problem. Rapid changes in velocity and pressure are assumed unidirectional, implying that the changes in mass, velocity and energy associated with a transient flow are more significant in axial direction than in radial direction. This provides a one-dimensional simplification of an initially complex problem, which computes fast and is easy to implement. The method utilizes characteristic lines to form a characteristic grid to compute the varying piezometric heads and discharges in a pipe segment for a given amount of time.

The characteristic equations are made up by the momentum and continuity equations, which both are nonlinear, first order partial differential equations:

$$\underbrace{g\frac{\partial H}{\partial x}+\frac{fV|V|}{2D}+V\frac{\partial V}{\partial x}+\frac{\partial V}{\partial t}=0}_{Momentum\ equation} \qquad (3.2.1)$$

$$\underbrace{V\frac{\partial H}{\partial x}+\frac{\partial H}{\partial t}+\frac{a^2}{g}\frac{\partial V}{\partial x}=0}_{Continuity\ equation} \qquad (3.2.2)$$

g is the acceleration of gravity, H is the piezometric head, x is the axial direction of the pipe, f is the pipe friction factor, D is the pipe diameter, V is the velocity of the flow, t is the time and a is the wave speed. The advective terms $V\,\partial V/\partial x$ and $V\,\partial H/\partial x$ are insignificant compared to the other terms and can be neglected. Eq. (3.2.1) and Eq. (3.2.2) are then simplified to

$$g\frac{\partial H}{\partial x}+\frac{fV|V|}{2D}+\frac{\partial V}{\partial t}=0 \qquad (3.2.3)$$

$$\frac{\partial H}{\partial t}+\frac{a^2}{g}\frac{\partial V}{\partial x}=0 \qquad (3.2.4)$$

The final C^+ and C^- characteristics lines are obtained by a linearization of the functions. The computational procedure is given in *Appendix C*.

$$C^+\ equation: \quad \begin{cases} \frac{g}{a}\frac{dH}{dt}+\frac{dV}{dt}+\frac{fV|V|}{2D}=0 \\ for\ \frac{dx}{dt}=a \end{cases} \qquad (3.2.5)$$

$$C^-\ equation: \quad \begin{cases} \frac{g}{a}\frac{dH}{dt}-\frac{dV}{dt}-\frac{fV|V|}{2D}=0 \\ for\ \frac{dx}{dt}=-a \end{cases} \qquad (3.2.6)$$

$dx/dt = a$ and $dx/dt = -a$ denote the slopes of the C^+ and C^- equations, respectively. The wave speed remains constant in a single pipe segment with constant properties, but varies with changes in pipe material and geometry. For a pipe of a given length, the characteristic lines provide new values of the discharge and head for a chosen number of time steps Δt. The characteristic procedure is explained in terms of the x-t grid illustrated in Figure 3-1:

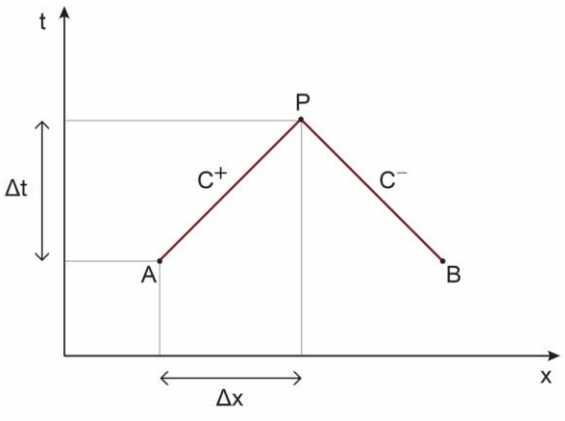

Figure 3-1: x-t grid. Definition of characteristic lines

The nodes A and B represent the head and flow conditions at a given time t and P denotes

the node in between, one time step ahead. The pipe is divided into N nodes and the distance between each node for a pipe length L is given by:

$$\Delta x = \frac{L}{N} \qquad (3.2.7)$$

Δt and Δx are related to each other and the wave speed by the following expression:

$$\Delta t = \frac{\Delta x}{a} = \frac{L}{aN} \qquad (3.2.8)$$

Δt depends on the choice of N, the length of each pipe segment and the wave speed and must be evaluated carefully in cases with several pipes and various properties. The more nodes chosen in the characteristic operation, the smaller Δt becomes. A general, numerical solution of the characteristic procedure is summarized in Figure 3-2.

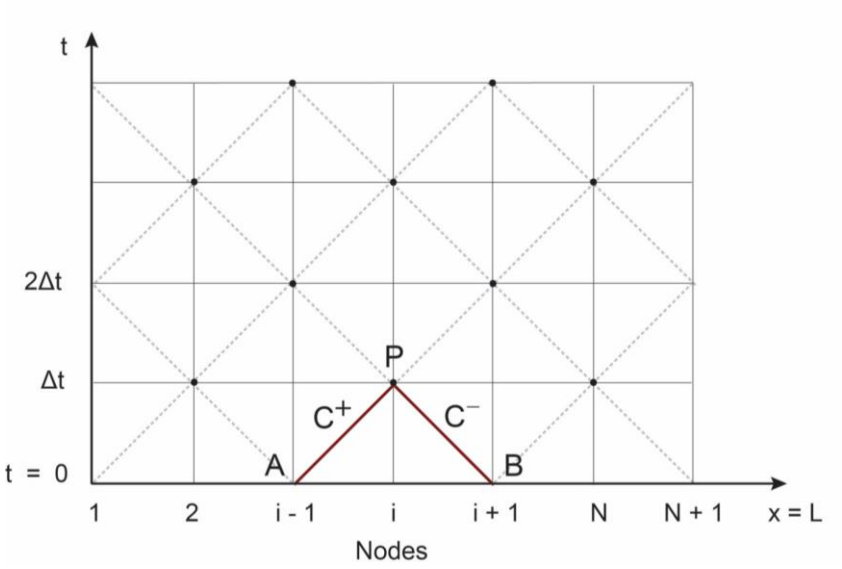

Figure 3-2: Characteristic grid. Solution of the C^+ and C^- equations.

i represents the node to be calculated, while $i-1$ and $i+1$ are the nodes downstream and upstream node i, respectively. The node at the pipe end is denoted $N+1$, often referred to as NS.

3.3 Numerical procedure

The characteristic C^+ and C^- lines are solved numerically by a reformulation of the original characteristics. The following numerical considerations are based on the procedures formulated by J. Tullis (Tullis, 1989). By expressing the characteristic equations in terms of the flow rate Q, related to the mean velocity by $Q = AV$, the numerical equations become:

$$C^+: \; HP_i - H_{i-1} + B(QP_i - Q_{i-1}) + R\, Q_{i-1}|Q_{i-1}| = 0 \qquad (3.3.1)$$

$$C^-: \; HP_i - H_{i+1} - B(QP_i - Q_{i+1}) - R\, Q_{i+1}|Q_{i+1}| = 0 \qquad (3.3.2)$$

The flow and head at a given time are referred to as Q and H, while the unknown flow and head one time step later are referred to as QP and HP. B denotes the characteristic impedance of the pipeline and is defined as:

$$B = \frac{a}{gA} \qquad (3.3.3)$$

R represents the frictional losses and is described by means of the Darcy friction factor when constant friction is assumed:

$$R = f\frac{\Delta x}{2gDA^2} \qquad (3.3.4)$$

Expressing the characteristic functions in terms of CP and CM, yields a simplified representation of Eq. (3.3.1) and Eq. (3.3.2):

$$C^+: \; HP_i = CP - B\, QP_i \qquad (3.3.5)$$

$$C^-: \; HP_i = CM + B\, QP_i \qquad (3.3.6)$$

Since the final head HP_i is common for both of the characteristics in Eq. (3.3.5) and Eq. (3.3.6), a final solution for the head and discharge is found by a combination of the equations:

$$HP_i = \frac{(CP + CM)}{2} \qquad (3.3.7)$$

$$QP_i = \frac{CP - HP_i}{B} \qquad (3.3.8)$$

The Brunone unsteady friction model discussed in Eq. (2.4.1) may be included in the momentum equation Eq. (3.2.3) to account for the unsteadiness, by neglecting the convective acceleration term:

$$\frac{\partial H}{\partial x} + \frac{1}{g}\frac{\partial V}{\partial t} + \left[f_q \frac{V|V|}{2gD} + \frac{k}{2g}\left(\frac{\partial V}{\partial t}\right)\right] = 0 \qquad (3.3.9)$$

The characteristic equations with quasi-steady and unsteady pressure loss terms become:

$$C^+: \; HP_i = H_{i-1} - B(QP_i - Q_{i-1}) - \left(f_q \frac{Q_{i-1}|Q_{i-1}|}{2gDA^2} + \frac{k}{2gA}\left(\frac{\partial Q_i}{\partial t}\right)\right)\Delta x \qquad (3.3.10)$$

$$C^-: \; HP_i = H_{i+1} + B(QP_i - Q_{i+1}) + \left(f_q \frac{Q_{i+1}|Q_{i+1}|}{2gDA^2} + \frac{k}{2gA}\left(\frac{\partial Q_i}{\partial t}\right)\right)\Delta x \qquad (3.3.11)$$

The temporal acceleration is numerically computed by:

$$\frac{\partial Q_i}{\partial t} = \frac{QP_i - Q_i}{\Delta t} \qquad (3.3.12)$$

Since QP is unknown, an iterative process is required to find the acceleration term $\partial Q/\partial t$ at each node and time step.

3.4 Boundary conditions

The application of the method of characteristics is useful when considering a simple, straight pipeline with a reservoir positioned at node 1 and a closing valve positioned at node $N + 1$. It is sufficient to apply boundary conditions for the flow and head at the reservoir and valve, assuming constant geometry and properties along the pipe:

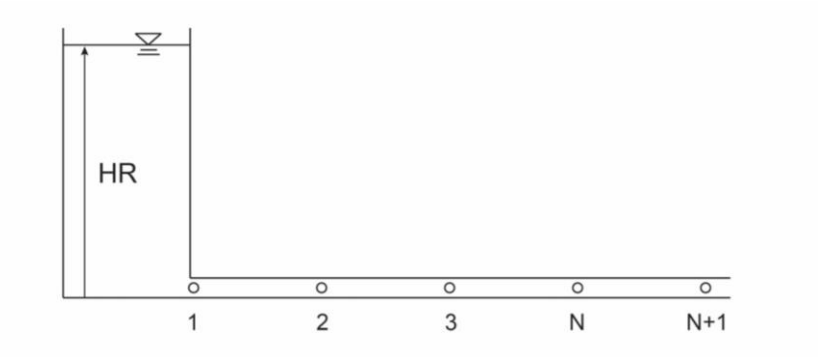

Figure 3-3: Representation of a simple 1-D pipeline with one reservoir and valve

3.4.1 Boundary conditions at the reservoir

By assuming no changes in the reservoir level, the head remains constant throughout the valve closure:

$$HP_1 = HR \qquad (3.4.1)$$

QP_1, on the other hand, depends on the change of flow rate and decreases until the valve is completely shut off. The change in QP_1 is determined by:

$$QP_1 = \frac{CP - HP_1}{B} \qquad (3.4.2)$$

3.4.2 Boundary conditions at the valve

Until the valve is closed, the flow and head depend on the valve opening and the reservoir head $HR2$ downstream the valve. By applying the energy equation between the reservoir

and the valve, an expression of the head at the valve is found equal to

$$HP_{N+1} = HR2 + C3\ Q_{i+1}|Q_{i+1}| \qquad (3.4.3)$$

The constant $C3 = K_v/(2gA_v^2)$, where A_v is the valve area and K_v is the valve loss coefficient. K_v can be obtained from the flow coefficient c_d by the relation:

$$K_v = \frac{1}{C_d^2} - 1 \qquad (3.4.4)$$

The flow coefficient depends on the valve type, the flow and valve opening and varies throughout the valve closure. From Eq. (3.3.5), the C^+ characteristic provides a second expression for the downstream head:

$$HP_{N+1} = CP - B\ QP_{N+1} \qquad (3.4.5)$$

By combining Eq. (3.4.3) and Eq. (3.4.5), the equations yield a quadratic equation for the discharge at the final node QP_{N+1}:

$$QP_{N+1}|QP_{N+1}| + \frac{B}{C3}QP_{N+1} + \frac{HR2 - CP}{C3} = 0 \qquad (3.4.6)$$

Solved by:

$$QP_{N+1} = 0.5\left(-\frac{B}{C3} \pm \sqrt{\left(\frac{B}{C3}\right)^2 - 4\left(\frac{HR2 - CP}{C3}\right)}\right) \qquad (3.4.7)$$

The discharge QP_{N+1} is present in the pipeline until the valve is completely closed. After the closure, $QP_{N+1} = 0$ and the head $HP_{N+1} = CP$.

3.4.3 Evaluation of a complex pipe flow

For pipelines with varying areas, pipe materials and wave speeds, additional boundary conditions must be considered to achieve a proper characteristic solution. For a sudden

change in the pipe diameter, it is necessary to define the boundary conditions between the connected pipes. If no losses occur between pipe j and pipe $j+1$, both the head and flow remains constant in the transition area and the boundary conditions are expressed as:

$$HP_{j,N+1} = HP_{j+1,1} \qquad (3.4.8)$$

$$QP_{j,N+1} = QP_{j+1,1} \qquad (3.4.9)$$

The boundary conditions in a pipe connection is further explained in Figure 3-4:

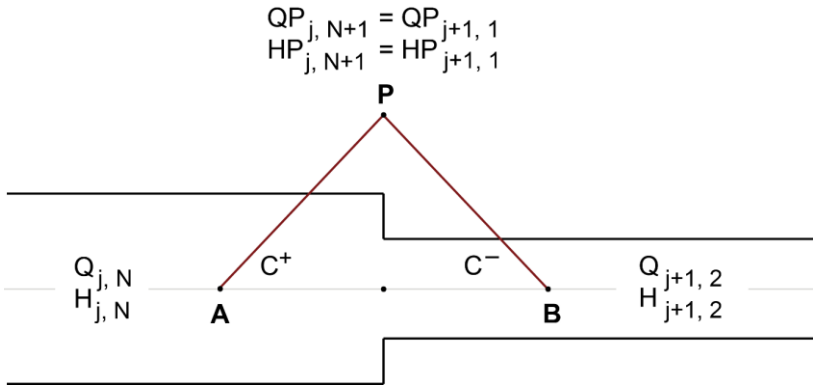

Figure 3-4: Numerical notations for a pipeline with sudden contraction.

3.4.4 Evaluation of the time step Δt

When dealing with complex pipe systems, the time step Δt must be considered to avoid inconsistency in head and flow throughout the pipeline. Having two different time steps in the simulation provides two different time frames, which is highly undesirable. As presented in Eq. (3.2.8), the time step depends on the pipe length, the wave speed and the number of nodes. Δt is adjusted by increasing or decreasing the number of nodes until reaching the desired value or by adjusting the pipe lengths slightly. This is usually not sufficient and a slight discrepancy between the time steps remains present. However, given that the value of wave speed is quite uncertain, some variation of it is allowed, as discussed in paragraph 3.1.

4 Material and methods

4.1 Experimental setup

Absolute pressure-time measurements were carried out in the Waterpower Laboratory at NTNU during the spring of 2016. The validity of a preinstalled Gibson test rig was evaluated by performing a wide number of repetitions and by assessment of the measuring equipment (Dahl, 2016).

The concept behind the Gibson test rig in the Waterpower Laboratory is rather simple. A centrifugal pump located in the laboratory cellar pumps water up to a water tank positioned at the attic. A narrow water channel connects the tank receiving water from the pump and a tank that represents the pressure head. A regulation device is installed in both tanks, allowing for an adjustment of the reservoir level and provides a maximum pressure head of approximately 9.75 m. Further, the water is led down to a long, straight pipe arranged with pressure taps suited for execution of pressure-time measurements. The test pipe is made of stainless steel with a length of 26.67 m and an inner diameter of 0.3 m, as seen in the illustration in Figure 4-1. A knife gate is installed at the end of the pipe and is connected to a hydraulic aggregate, which enables a thoroughly controlled closure of the valve during the measurements.

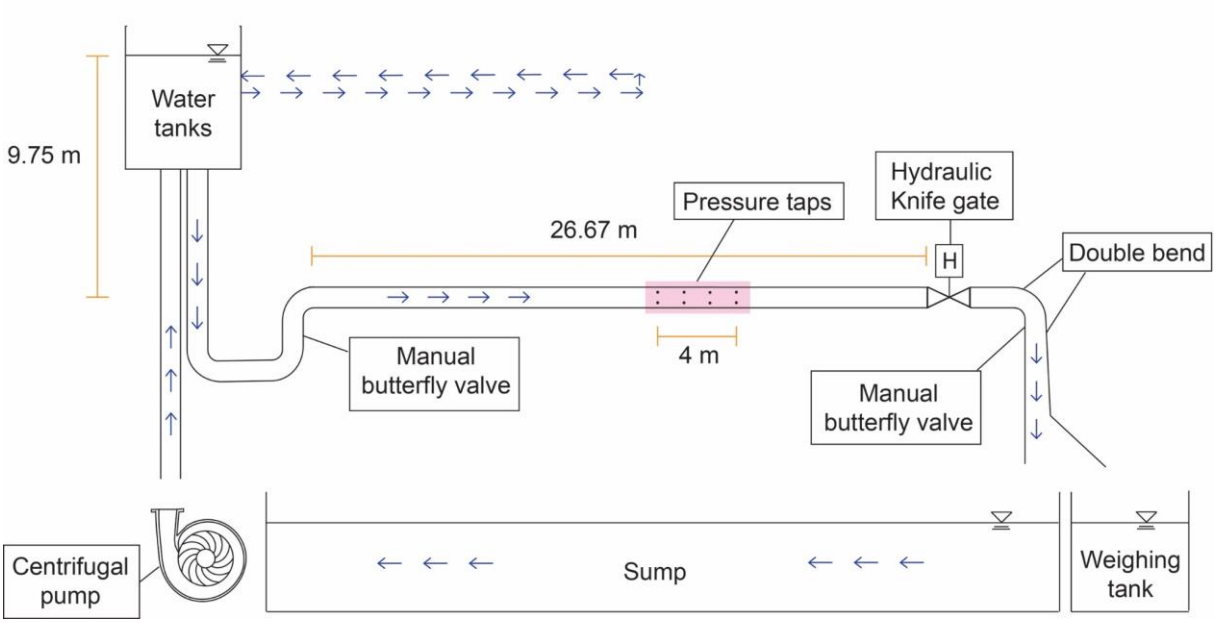

Figure 4-1: Setup of the Gibson test rig in the Waterpower Laboratory at NTNU

Absolute pressure sensors *(UNIK 5000)* were used in the experiments with a pressure range of 0 to $5\ bar$ and an accuracy of $\pm 0.04\ \%$. They were installed on the test pipe with a spacing of 4 m, 10 meters upstream the gate valve. The IEC 41 (1991) recommend use of differential pressure sensors with tubing, but due to faulty of the differential sensors available, absolute sensors were applied instead. The sensors were calibrated using a pneumatic deadweight tester *(Fluke Calibration P3000)* suited for calibration between 0.2 and $35\ bar$. The accuracy of the deadweight tester is 0.008 % of reading. A highly accurate electromagnetic flowmeter *(KROHNE IFS 4000)* with a measuring error of $0.3\ \%$ was used as a reference flow for validation of the pressure-time calculations. The data obtained from the electromagnetic flowmeter, the pressure sensors and the valve position were digitalized via a DAQ and recorded and sampled using the logger program *NI Signal Express.*

Laboratory pressure-time measurements were carried out for two test cases with flow rates approximately equal $170\ l/s$ and $400\ l/s$. This corresponds to VL relations of $9.64\ m^2/s$ and $22.64\ m^2/s$, respectively, which are far below the requirement stated in the IEC 41 (1991) standard. The pipeline geometry between the reservoir and the test area is rather complex, as it contains several bends, valves, dead ends, contractions and expansions. The test section had to be positioned as close to the knife gate as possible to avoid the disturbances from the geometry variations. However, some distance from knife gate was also necessary to withstand the effects caused by a double bend installed downstream the valve.

The hydraulic aggregate controlling the closure was managed by a *LabView* control program, which allowed for several repetitions of the pressure-time measurements to be executed automatically. Slight variations in the response of the hydraulic aggregate was detected and caused some discrepancies between the measurements. The average closure times were approximately 4.6 s and 4.7 s for the flows at $170\ l/s$ and $400\ l/s$, respectively. MATLAB was used for as a mathematical tool during post processing the measuring data.

Since no leakage flow was discovered in the pipeline after shut off, the leakage term in the pressure-time integral was irrelevant to evaluate.

4.2 Evaluation of the absolute pressure-time integral

The discharge in the Gibson test pipe was evaluated using both the constant friction and the quasi-steady approach and was assessed by comparison with the installed electromagnetic flowmeter. The pressure-time integral was solved using the MATLAB built-in function *cumtrapz*. This function uses the principle behind the trapezoidal method to determine the area enclosed by the differential pressure and the pressure recovery line. It provides a vector with the cumulative integral of the differential pressure as a function of time. The final pressure-time flow was found by taking the average over a wide range of sample points, due to the incidence of small oscillations in the final integral, as discussed in paragraph 2.1.1. For each iteration step, a new value of the pressure-time flow was calculated and transmitted to the next iteration until a preset simulation tolerance was reached.

An initial start value of the flow rate was needed in order to initiate the computation and was found by assuming linear losses. The linear pressure losses were implemented in the sampled pressure data as shown in Figure 4-2:

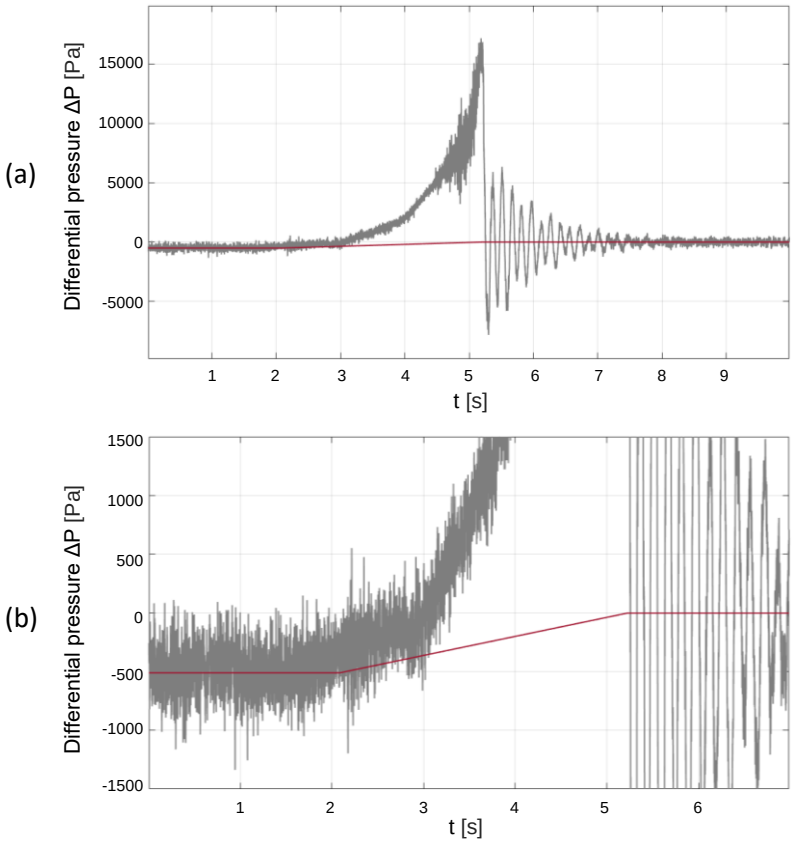

Figure 4-2: Linear pressure losses implemented into an aboslute differential pressure. (a) Full scale figure. (b) Enlarged section of the linear loss.

The initial linear losses equal the initial differential pressure and decreases linearly until reaching the static line end, where the losses are assumed zero. This is a reasonable assumption since the frictional effects are small, almost negligible after closure. Finding the area between the differential pressure curve and the linear pressure losses provides the needed start value of the flow rate Q.

4.2.1 Constant friction implementation

The pressure losses were calculated using the Darcy-Weisbach equation by assuming constant friction, as discussed in paragraph 2.3.1. The initial Reynolds number was found using the flow from the linear assumption and the inner diameter and cross-sectional area of the constant pipe section. Furthermore, the constant friction factor was estimated using the Colebrook-White formula and included in the Darcy-Weisbach equation (2.2.1). The iterative procedure of the pressure loss ξ_{n+1} is presented numerically in the following equation:

$$\xi_{n+1} = \mathrm{f}\frac{L}{D}\frac{\rho}{2A^2} \cdot (Q_{n+1} - \bar{Q}_n)|(Q_{n+1} - \bar{Q}_n)| \qquad (4.2.1)$$

where ξ_{n+1} and Q_{n+1} are vectors containing information about the pressure losses and flows at each time step and $\overline{\mathrm{Q}}_n$ is the value of the final pressure-time flow calculated in the previous iteration. The losses were included in the pressure-time integral and solved by the *cumtrapz* function at each iteration point.

4.2.2 Quasi-steady friction implementation

When assuming quasi-steady friction, a computation of the losses are conducted at each time step throughout the measurement, as concluded in paragraph 2.3.1. The initial value of k_2 was found by the differential pressure $\Delta P = P_2 - P_1$ and the initial value of Q was determined by the linear assumption. During the iteration process, new values of k_2 and Q were accumulated until a preset toleration of the iteration was reached. Two similar approaches were considered when solving the relation $\xi(\mathrm{t}) = k_2 \cdot Q(t)|Q(t)|$:

$$\xi_{n+1} = k_2 \cdot (Q_{n+1}^2 - \bar{Q}_n^2) \qquad (4.2.2)$$

$$\xi_{n+1} = k_2 \cdot (Q_{n+1} - \bar{Q}_n)|(Q_{n+1} - \bar{Q}_n)| \qquad (4.2.3)$$

Eq. (4.2.2) yields the difference in losses between the current flow vector and the flow at the previous time step, while Eq. (4.2.3) calculates the losses created by the flow differences. Both approaches provided somewhat similar results, but the second approach was applied in further investigations of the pressure-time flow. Eq. (4.2.2) looks at the difference in losses by assuming equal loss constant for both flows. k_2 is highly dependent on the flow at each iteration step, which could possibly contribute to some discrepancies by use of the method. Moreover, simulations revealed a considerable larger spread in the final pressure-time flows when using Eq. (4.2.2) instead of Eq. (4.2.3).

4.3 Evaluation of the relative pressure-time integral

4.3.1 Preparation of relative the measurements

The relative pressure-time method was evaluated using the experimental data obtained from the absolute measurements. The relative test section was extended to include the pipeline located between the water tank and the test section 10 m upstream the valve. The relative setup in the Gibson test pipe is further explained in Figure 4-3.

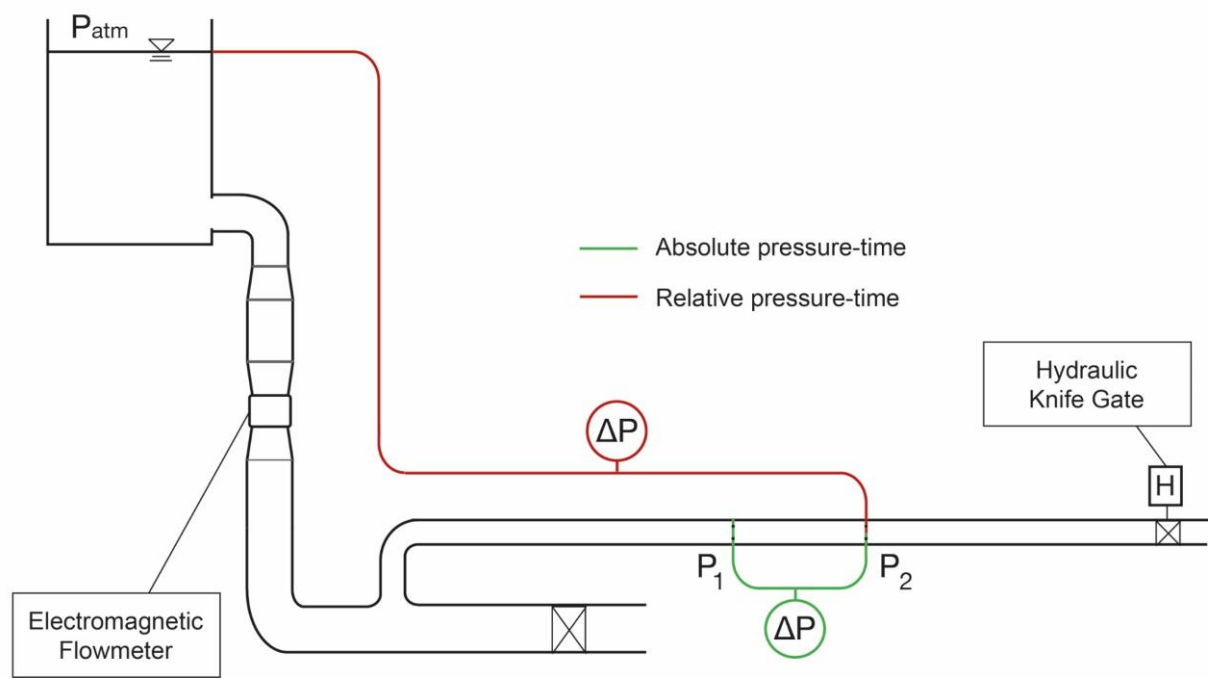

Figure 4-3: Differential pressure sections for absolute and relative measurements in the Waterpower Laboratory.

By utilizing the atmpostheric pressure at the surface of the water tank, the differential pressure in the extended test section was found by:

$$\Delta P = P(t) - P_{atm} \qquad (4.3.1)$$

where $P(t)$ represents the time-dependent pressure measured by pressure sensor 2 and P_{atm} denotes the constant atmospheric pressure at the reservoir. The main challenge of calculating the relative pressure-time integral is to find a good approach to the pipe factor in the system, as previously discussed. Since the geometry of the relative test section includes several bends, contractions and expansions, the effects originating from the minor losses must be considered in addition to the frictional losses. Moreover, the relative Gibson

pipeline includes two dead ends, which must be considered in the evaluation of the pipe factor.

The concept behind the relative pressure-time integral was discussed in paragraph 2.5 and the issue regarding the unknown pipe geometry and the losses was introduced. A possible technique of determining the geometrical constant k_1 was briefly discussed and a computational approach was suggested. It should be possible to obtain a good approximation of the pressure loss constant k_2 if succeeding in the evaluation of the geometrical constant.

4.3.2 Calculation of the geometrical constant $\boldsymbol{k_1}$

The pipe factor of a pipeline is defined as the summation of all local pipe factors along the pipeline (Adamkowski et al., 2008):

$$F = \sum_{i=1}^{n} \frac{L_i}{A_i} = \frac{L_1}{A_1} + \frac{L_2}{A_2} + \cdots + \frac{L_n}{A_n} \qquad (4.3.2)$$

where n denotes the number of pipe segments and L_i and A_i are the length and cross-sectional area of each pipe segment.

Calculation of the pipe factor was done by utilizing the dimensions of the Gibson test pipe. The water reservoir was not accounted for, by assuming a low flow velocity. The pipe factor was calculated from the outlet of the reservoir to pressure sensor P, as illustrated in Figure 4-4:

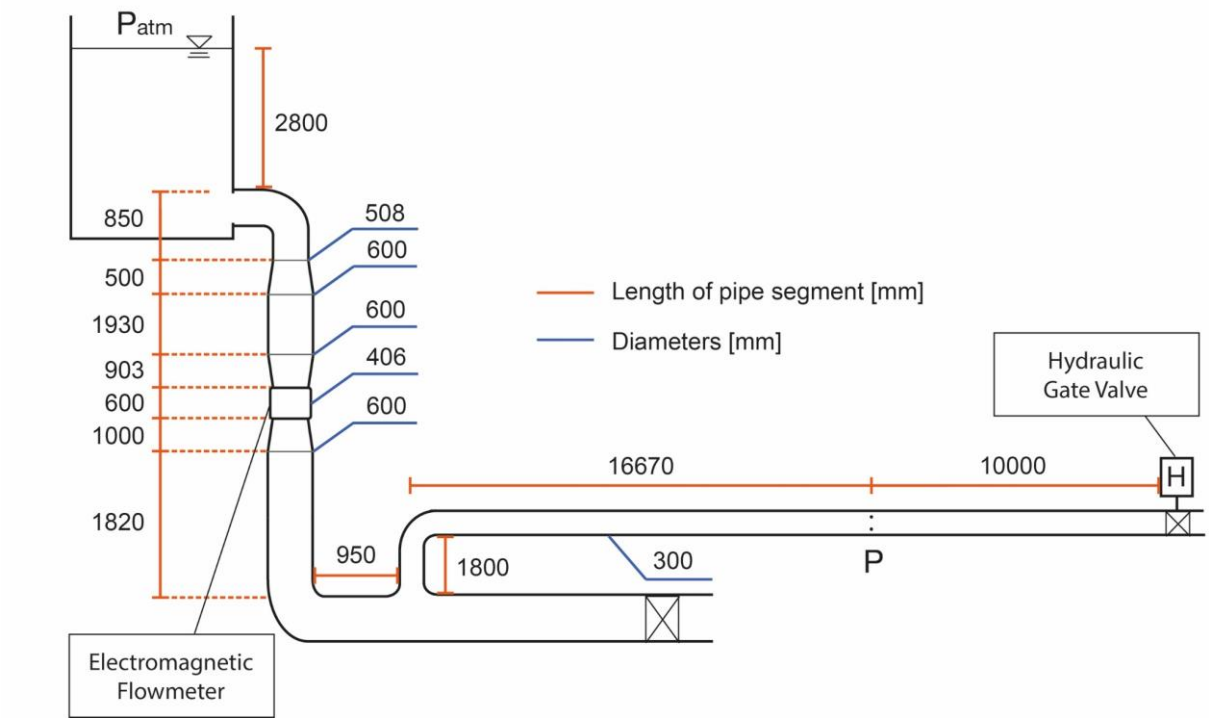

Figure 4-4: The dimensions of the Gibson test pipe

Moreover, the bends were excluded for a simplification of the problem. Geometrical variations due to pipe contractions and expansions were accounted for by dividing the pipes segments into tiny sections and separately calculating the pipe factor of each piece. The dead ends appearing in the pipeline were treated as a fixed wall. By assuming internal circulation inside a dead end, described by the streamlines shown in Figure 4-5, the outermost circulating streamline may be regarded as a solid wall for the passing pipe flow. The assumption presumes a steady, incompressible flow.

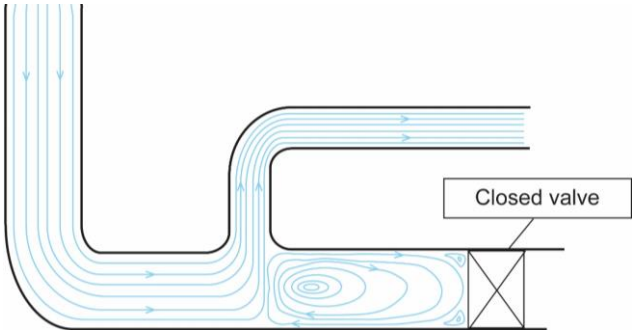

Figure 4-5: Assumed circulation of internal streamlines in a dead end.

All individual friction factors were summarized and included in Eq. (2.5.1) to yield a value of the geometrical constant k_1:

$$k_1 = \frac{1}{\rho F}$$

4.3.3 Evaluation of the loss constant k_2

The procedure of calculating the relative pressure losses is similar to the absolute quasi-steady method. Due to the occurrence of minor losses in the pipeline, the loss constant k_2 must represent both minor and frictional losses, as formulated in Eq. (2.2.5). Similar to the absolute quasi-steady approach, the initial loss ξ_0 must be determined by the initial differential pressure and k_2 must be included in the iterative process to determine the final relative flow. The final value of k_2 depends on the choice of the geometrical constant, as briefly mentioned in paragraph 2.5.

A complex problem arises during the iteration process of finding the relative pressure-time flow, represented graphically in Figure 4-6.

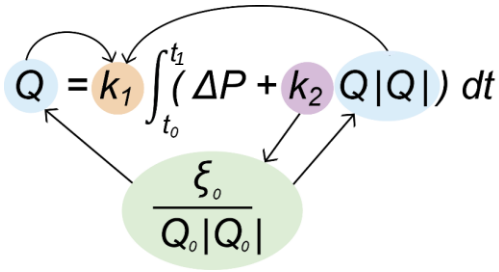

Figure 4-6: Interaction between the parameters during an iteration.

The figure describes the parameters that depend on each other. The loss coefficient k_2 depends on the initial pressure loss ξ_0 and the initial flow rate Q_0, which in turn depends on the calculated pressure-time flow. k_1 is a fixed constant in front of the pressure-time integral, implying that the choice of k_1 has a great impact on the final flow and hence the losses at each iteration step.

In order to examine the effects of choosing various geometrical constants, the repeatability between the relative measurements was investigated by calculating the ratio Q_{400}/Q_{170} for a wide range of various k_1. In case of considerable discrepancies between the ratios, the presented pressure-time method may prove to be invalid for relative analysis. An opposite case will, however, prove the method's ability to repeat the measurements for two arbitrary flows, regardless of the choice of k_1.

4.3.4 The procedure of finding the relative pressure-time flow

As for the absolute pressure-time procedure, the relative integral in Eq. (2.5.2) was solved using the MATLAB trapezoidal function *cumtrapz.* The following equation explains how the *cumtrapz* function was included in the iterative process:

$$Q_{n+1} = k_1 \cdot \ cumtrapz\ (t, \Delta P + k_2 \cdot (Q_{n+1} - \bar{Q}_n)|(Q_{n+1} - \bar{Q}_n)|) \qquad (4.3.3)$$

n and $n+1$ represent the previous iteration step and the current step, respectively. t is a vector containing the time scale of the measurements and ΔP holds the corresponding differential pressure at each time step. Q_{n+1} is a vector containing the cumulative computation of the pressure difference with respect to t and $\bar{Q}_n$ is the final flow value, calculated from the previous flow vector Q_n.

The tolerance of the iteration process was set to 10^{-14} to ensure that the calculation was entirely completely. For each iteration step, the difference between the old and the new value of the pressure-time flow was compared to the tolerance. The iteration continued until the difference was sufficiently small.

A flow chart of the iteration procedure is shown in Figure 4-7 and the associated MATLAB script is attached in *Appendix A*.

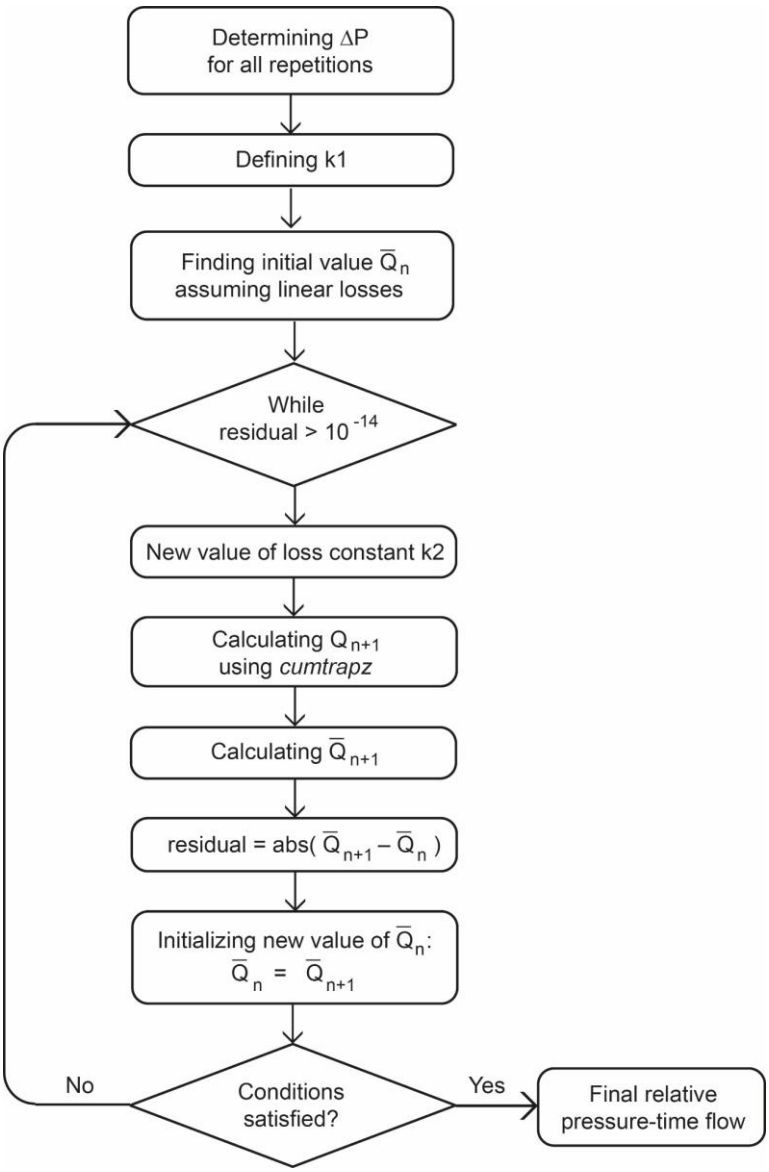

Figure 4-7: Flow chart explaining the relative flow iteration.

4.4 Numerical setup

4.4.1 Introduction of the test cases

Two different numerical cases were made to verify the relative experimental results. The first case represents a simple pipeline with constant geometry, while the second represents a complex pipeline with a sudden contraction.

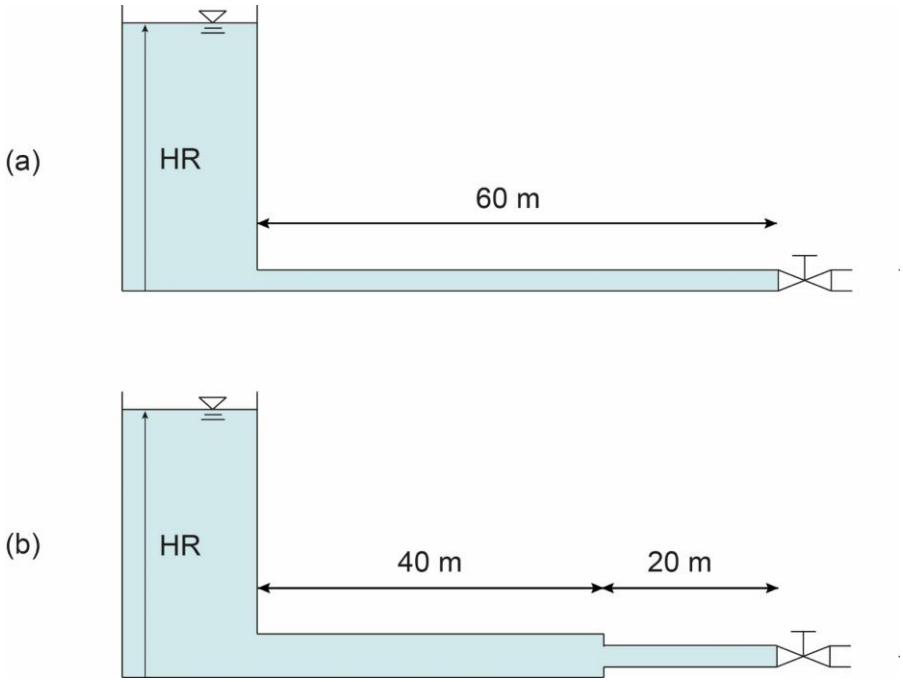

Figure 4-8: Numerical test cases: (a) Simpel, straight pipe. (b) Complex pipe.

The simple pipeline, illustrated in Figure 4-8 (a), consists of a reservoir, a straight pipe and a closing valve. The number of nodes was chosen to 25, providing a time step of $\Delta t = 0.0027\ s$, and the wave speed was estimated to be approximately $900\ m/s$. The gate was closed linearly from a fully open position to complete shut-off with a closure time $t_c = 4\ s$. The reservoir level was chosen to $4\ m$, and the straight pipe had an inner diameter of $0.3\ m$ and a pipe length of $60\ m$.

The complex pipeline ((b) in Figure 4-8) was given the same properties as the simple pipeline regarding the reservoir level, pipe length and closure time. However, the pipe was divided into two pipe segments with various diameters, lengths and nodes. The first segment was 40 m long with a diameter of 0.5 m, divided into 16 nodes. The second segment was 20 m, had a diameter of 0.3 m and 8 nodes. The wave speed was calculated to $900\ m/s$ and the time step was ensured equal to the time step of the simple case.

4.4.2 Valve characteristics

The valve characteristics are highly dependent on the flow rate and the differential pressure and had to be found for each flow in terms of the dimensionless flow coefficient c_d, as mentioned in paragraph 3.4. The coefficients chosen for the numerical cases are plotted as a function of the valve opening in Figure 4-9:

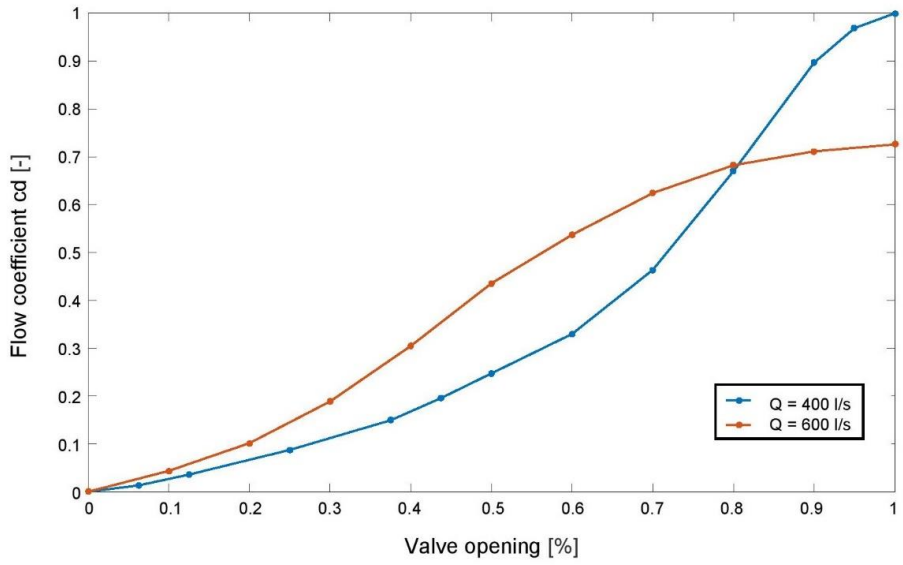

Figure 4-9: Valve characteristics applied in numerical model

4.4.3 Building the code

The numerical codes for both test cases were written almost identical. Some extra lines were added to the complex code to describe the transition area between the pipe segments and to account for the various pipe properties.

The first step in the numerical script was to define the initial conditions, which included the pipe geometries, the initial flow rate, the time step, the number of nodes and the wave speed. Further, the gate closure time and the duration of the simulation were set and the initial values of the discharge and head were defined. The simulations were then carried out inside a while loop until the preset time criterion was reached.

The frictional losses were described by implementation of the Brunone friction model, presented in Eq. (3.3.9). For each node at each time step, the quasi-steady and the unsteady friction factors were calculated and implemented into the pressure loss term. The quasi-steady frictions were found by the Colebrook-White equation (Eq. (2.2.3)) and the unsteady frictions were determined by an iterative approach. The iteration procedure is

further explained in the flow chart illustrated in Figure 4-10, and the corresponding MATLAB script is attached in *Appendix D*. QP and HP are the conditions at the current time step, Q and H are the conditions at the previous time step and Q_{temp} is a temporary value of the flow during the iteration until the tolerance criterion is fulfilled.

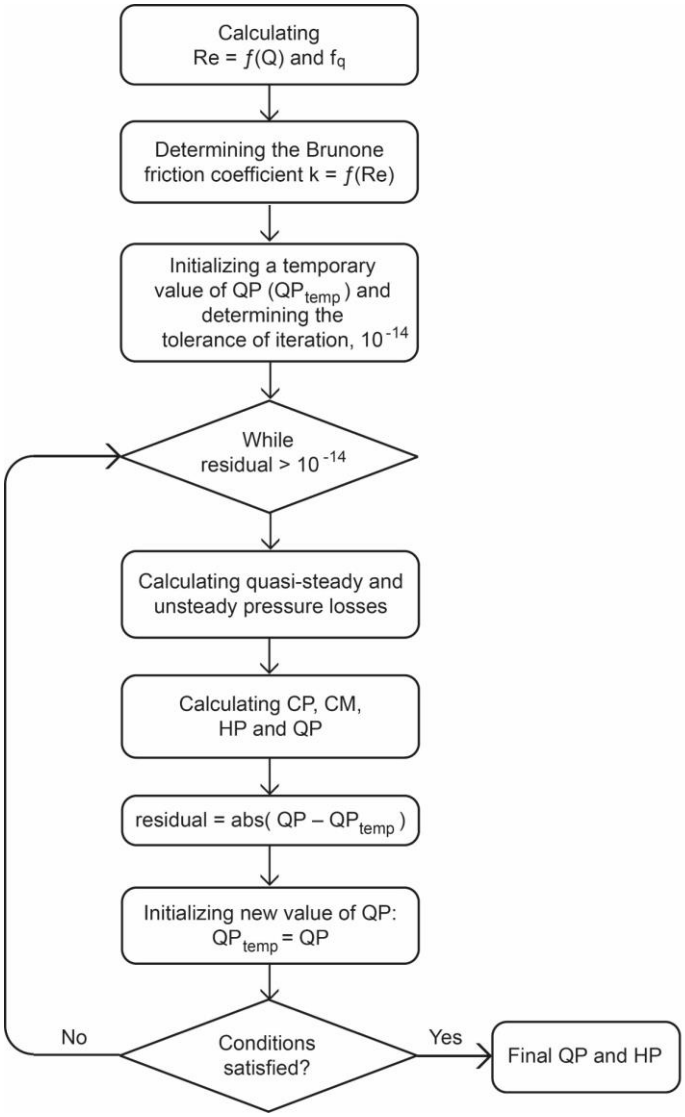

Figure 4-10: Iteration chart for pressure losses, QP and HP

The relative procedure explained in paragraph 4.3.4 was implemented into the numerical test cases for further calculations of the relative pressure-time flows.

5 Experimental results

5.1 Absolute measurements

A large number of repetitions were conducted for both test cases and the measurements were evaluated by including all valid data. The uncertainties presented in this section have been considered at a 95 % confidence level by the Student's t distribution. Due to the occurrence of outliers in the measurements, an additional statistical evaluation has been carried out to consider the effects of removed data.

Both test cases were conducted with gate closure times of approximately 4.6 s. A linear closure was carried out for the part load flow in test case 1. The closure of the flow in test case 2 was slow in the beginning and fast in the end in order to reduce the heavy impacts from the pressure fluctuations at the gate. The differential pressures obtained from the absolute pressure sensors are plotted in Figure 5-1 along with the valve position. Some of the conditions present during the absolute experiments are summarized in Table 5-1.

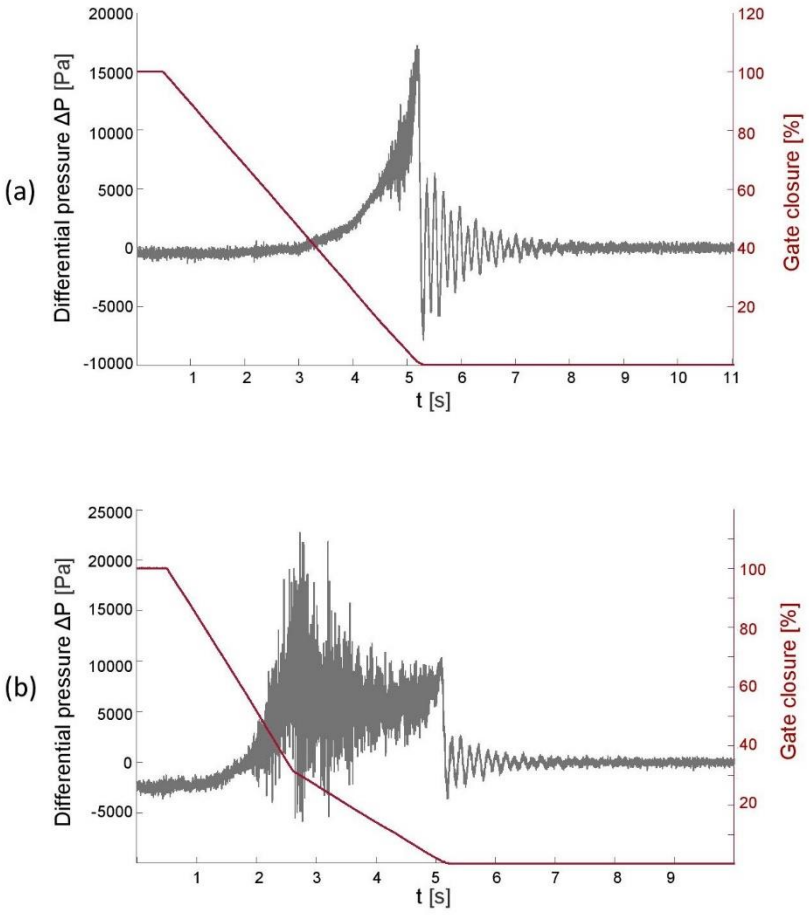

Figure 5-1: Differential pressures along with the valve closure position. (a) Test case 1. (b) Test case 2.

Test case:	**1**	**2**
Load:	43 %	100 %
Velocity V:	2.46 m/s	5.69 m/s
VL:	9.84 m^2/s	22.76 m^2/s
Number of repetitions:	38	46
Initial pressure loss ξ_0:	0.459 kPa	2.404 kPa
Pipe factor F:	56.6	56.6

Table 5-1: Conditions present during the absolute pressure-time measurements.

The reference flows obtained from the electromagnetic flowmeter were $0.1740\ m^3/s$ and $0.4020\ m^3/s$ for test case 1 and 2, respectively. Both flows were found as averages over a wide range of repetitions and examined by the Student's t distribution. The random errors were found equal to $0.0768\ \%$ and $0.0897\ \%$, which corresponds to uncertainties approximately 2 estimated standard deviations from the mean. Due to the incidence of low random errors, the reference flows are further considered in terms of their mean values. The statistical analysis is summarized in Table 5-2.

Test case:	**1**	**2**
Reference flow Q_{ref} :	0.1740 m^3/s	0.4020 m^3/s
Degrees of freedom:	37	45
Student's t:	2.03	2.02
Random uncertainty f_r:	0.000134	0.000361
Random error e_r:	0.0768 %	0.0897 %

Table 5-2: Random analysis of the reference flow.

Pressure-time flows were calculated considering both the quasi-steady friction and the constant friction. Both methods were incorporated in the pressure-time integrals for further computation of the discharge, as previous explained. The integrated pressure losses are plotted in Figure 5-2.

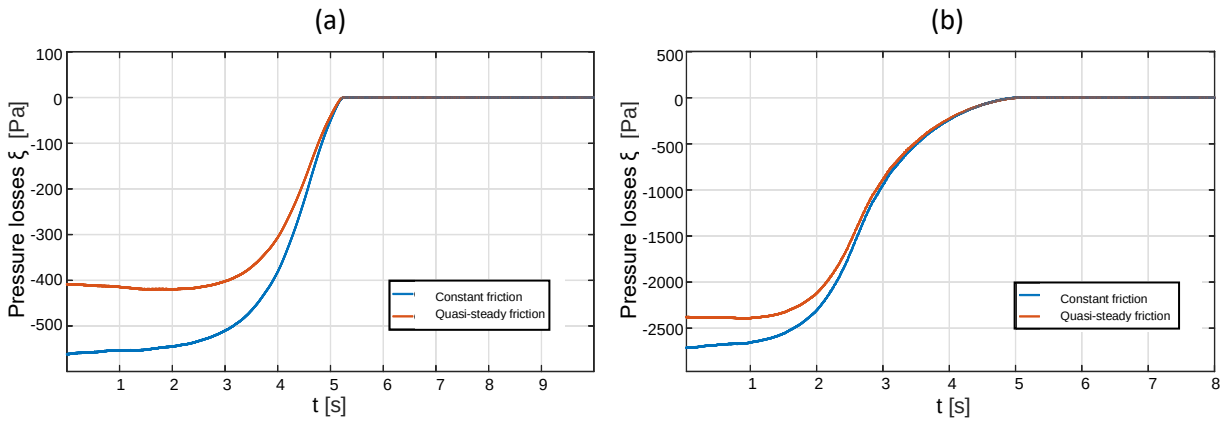

Figure 5-2: Iterated pressure losses using the quasi-steady and constant friction approach. (a) Test case 1. (b) Test case 2.

Application of the constant friction tends to contribute to a greater pressure loss than using the quasi-steady friction. The initial pressure differences between the methods are approximately 150 Pa and 330 Pa for test case 1 and 2, respectively. The results from the quasi-steady method and the constant friction method are discussed further by comparison with the reference flow.

5.1.1 Evaluation of the quasi-steady friction

The average pressure-time flows were calculated to $0.1713\ m^3/s$ and $0.4002\ m^3/s$ by the quasi-steady friction approach, with random errors of $0.520\ \%$ and $0.336\ \%$. All random uncertainties were calculated at a 95 % confidence interval using the Student's t distribution. The errors of the measurements when comparing with the flowmeter are presented in Figure 5-3. The random errors of the reference flows are not accounted for, as the mean values are assumed reasonable considering the large number of repetitions, as discussed in the previous section. The maximum discharge error of test case 1, calculated by means of Eq. (1.3.7), is close to $2.1\ \%$, while the corresponding value for test case 2 is 0.8 %.

One significant outlier was removed from test case 1, reducing the random error from $0.520\ \%$ to $0.477\ \%$. However, the result of removing one measurement led to a greater maximum discharge error. Two outliers were removed from the measurements in test case 2, providing a reduction in the random error from $0.336\ \%$ to $0.292\ \%$ and a further reduction in the discharge error. The removal of measurements appear reasonable due to the considerable reduction in the random errors by removing few outliers out of many repetitions. The flows calculated from the pressure-time integral using quasi-steady friction lies below the reference flow, implying a negative systematic error.

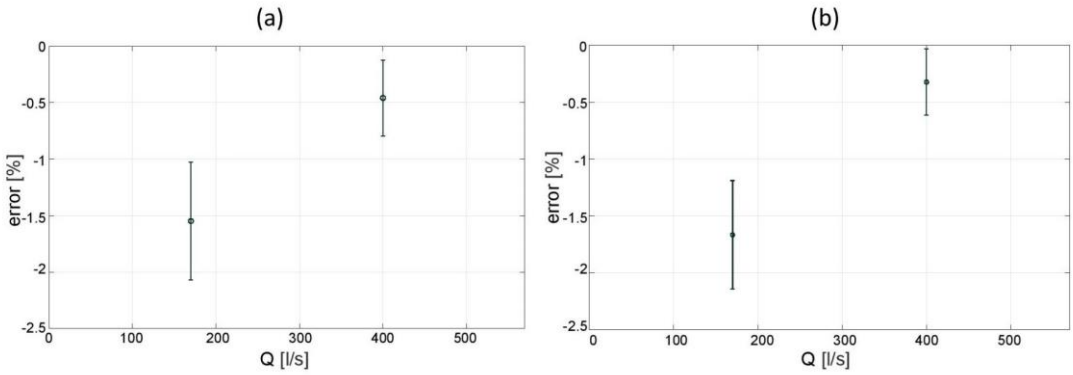

Figure 5-3: Discharge error of the pressure-time flow with a quasi-steady approach. Reference flow provided by an electromanetic flowmeter. (a) Origintal measurements. (b) Removed outliers.

The statistical considerations are summarized in Table 5-3:

Test case:	**1**	**2**
	Original results:	
Pressure-time flow Q:	0.1713 m^3/s	0.4002 m^3/s
Random uncertainty f_r:	$\pm$0.00089 m^3/s	$\pm$0.00134 m^3/s
Random error e_r:	0.520 %	0.336 %
Student's t:	2.032	2.021
Maximum discharge error e:	2.1 %	0.8 %
	Removal of outliers:	
Number of removed outliers:	1	2
Pressure-time flow Q:	0.1711 m^3/s	0.4007 m^3/s
Random uncertainty f_r:	$\pm$0.000816 m^3/s	$\pm$0.00117 m^3/s
Random error e_r:	0.477 %	0.292 %
Student's t:	2.034	2.024
Maximum discharge error e:	2.14 %	0.6 %

Table 5-3: Pressure-time results by applying quasi-steady friction on a confidence level of 95 %.

The discharge errors correspond well to the errors presented in P. Jonsson doctoral thesis (2011), as he calculated the pressure-time flows using a quasi-steady approach with a frictional constant k_2 calibrated from the initial pressure loss. Although his measuring length was 1 m shorter than the length presented in this thesis, he obtained maximum discharge errors of approximately 2.9 % for the flow at 2.4 m/s and 1 % for the flow at 5.8 m/s. However, lower random errors were obtained using the presented quasi-steady calculation method. The results appear to provide accuracies corresponding to Jonsson's measurements, but with a slightly higher precision.

5.1.2 Constant friction

The pressure-time calculations using the constant friction approach provided larger discharge errors for both flows, but the random errors were substantially smaller. Figure 5-4 shows maximum discharge errors of about 2.27 % and 2.47 % for test case 1 and 2. The random errors at the 95 % confidence level were found equal to 0.375 % and 0.201 %. Four measurements were removed from test case 1, decreasing the random error to 0.239 % and the discharge error to 2.08 %. The positive discharge errors in Figure 5-4 indicate positive systematic errors and an overestimation of both flows.

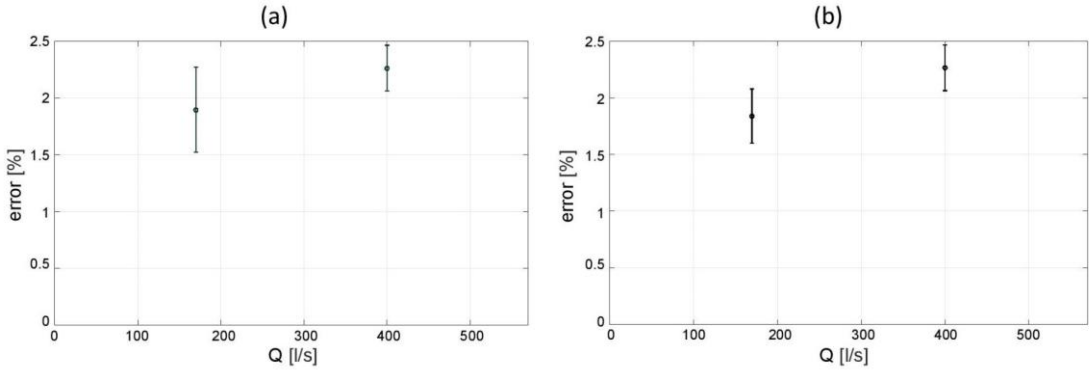

Figure 5-4: Discharge error of the pressure-time flow with a constant friction approach. Reference flow provided by an electromanetic flowmeter. (a) Origintal measurements. (b) Removed outliers.

Test case:	**1**	**2**
	Original results:	
Pressure-time flow Q:	0.1773 m^3/s	0.4111 m^3/s
Random uncertainty f_r:	$\pm$0.000666 m^3/s	$\pm$0.000828 m^3/s
Random error e_r:	0.375 %	0.201 %
Student's t:	2.032	2.021
Maximum discharge error e:	2.27 %	2.47 %
	Removal of outliers:	
Number of removed outliers:	4	0
Pressure-time flow Q:	0.1772 m^3/s	0.4111 m^3/s
Random uncertainty f_r:	$\pm$0.000423 m^3/s	$\pm$0.000828 m^3/s
Random error e_r:	0.239 %	0.201 %
Student's t:	2.038	2.021
Maximum discharge error e:	2.08 %	2.47 %

Table 5-4: Pressure-time results by applying constant friction on a confidence level of 95 %.

When comparing the constant friction results to the quasi-steady, the random errors are considerably lower. The accuracies, on the other hand, are much poorer, which contribute to substantially larger discharge errors.

5.2 Relative measurements

The differential pressures presented in Figure 5-5 are the relative pressures between the open reservoir and the pressure sensor. Since the atmospheric pressure remains constant throughout the measurement, the pressure distributions are simply just displacements of the original recorded pressures from the sensor. In the absolute method, two absolute pressure sensors were used to calculate the differential pressure in the measuring section, contributing to a large amount of noise in the signal, as shown in Figure 5-1. Hence, since only one sensor was applied in the calculation of the relative differential pressure, less noise is present.

(a)

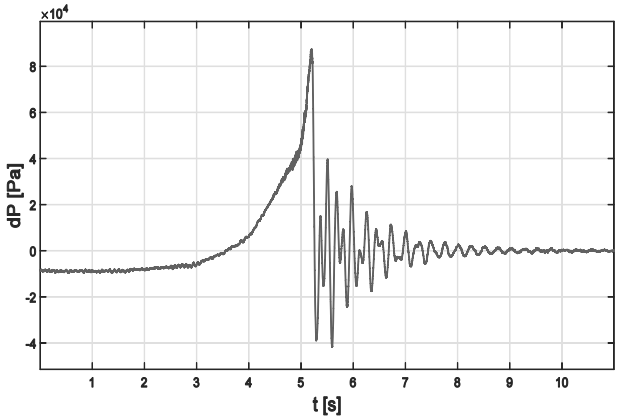

(b)

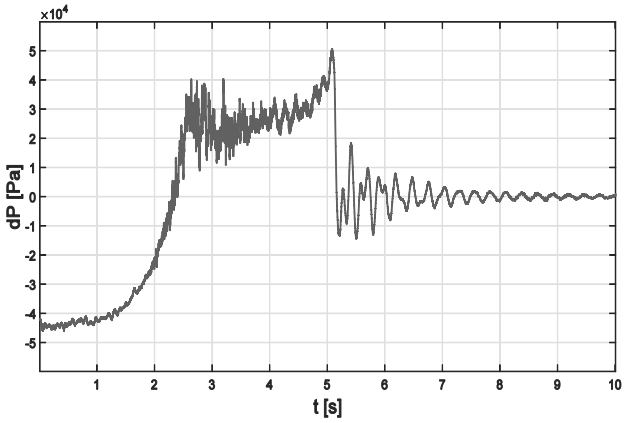

Figure 5-5: Differential pressures between the open reservoir and pressure sensor 10 m ustream the closing valve. (a) Test case 1. (2) Test case 2.

The initial pressure losses are considerably larger in the relative method, due to differences in heights between the measuring sections and due to a longer pipeline with various geometry. The mean values of the initial differential pressures are approximately equal -8800 and -44300 Pa for test case 1 and 2, respectively.

5.2.1 Computational value of the geometrical constant k1

In the process of calculating the geometrical constant, all pipe segments and areas were arranged in MATLAB for an individual calculation of the pipe factor. The pipe geometry stretching from the outlet of the reservoir to the pressure sensor 10 m upstream the knife gate is illustrated in Figure 5-6, with pipe cross-sectional areas as a function of the pipe length. When excluding the reservoir, the total pipe length is approximately 28 m. The geometrical variations are considerable in the beginning of the pipeline as shown in Figure 5-6, which represent the enlargements and contractions on the pipeline just downstream the outlet of the reservoir. The final simple pipe geometry in the figure represents the long straight pipe section upstream the knife gate.

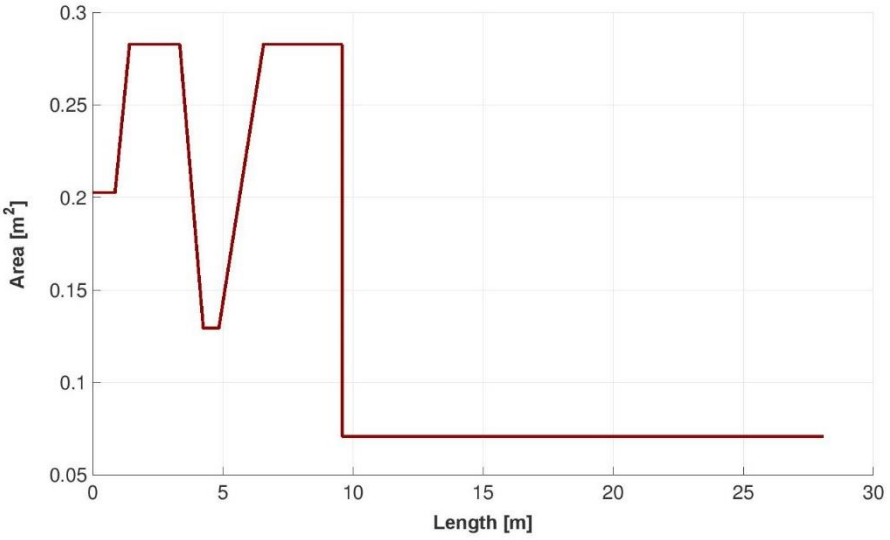

Figure 5-6: Variation in the pipe geometry.

By application of Eq. (4.3.2), the total pipe factor was found equal to $F = 303.094$, which corresponds to a geometrical constant equal $\mathrm{k}_1 = 3.2993 \cdot 10^{-6}$. The obtained geometrical constant was included in the relative pressure-time integral for further calculations of the relative flow. The cumulative computation of the flows as a function of time is plotted in Figure 5-7. The associated calculated pressure losses are shown in Figure 5-8.

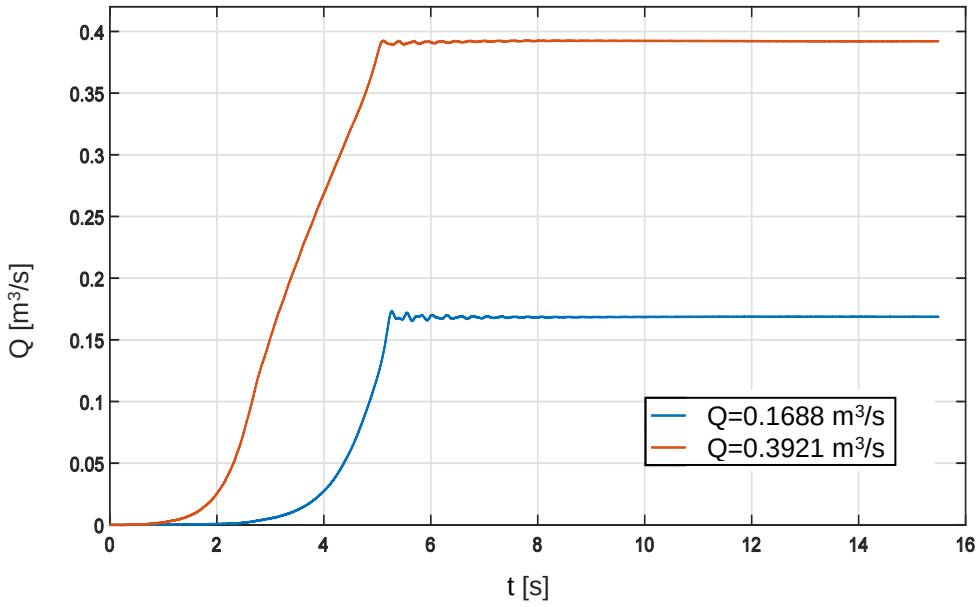

Figure 5-7: Integrated, cumulative solution using relative pressure-time method for the computational value of k_1.

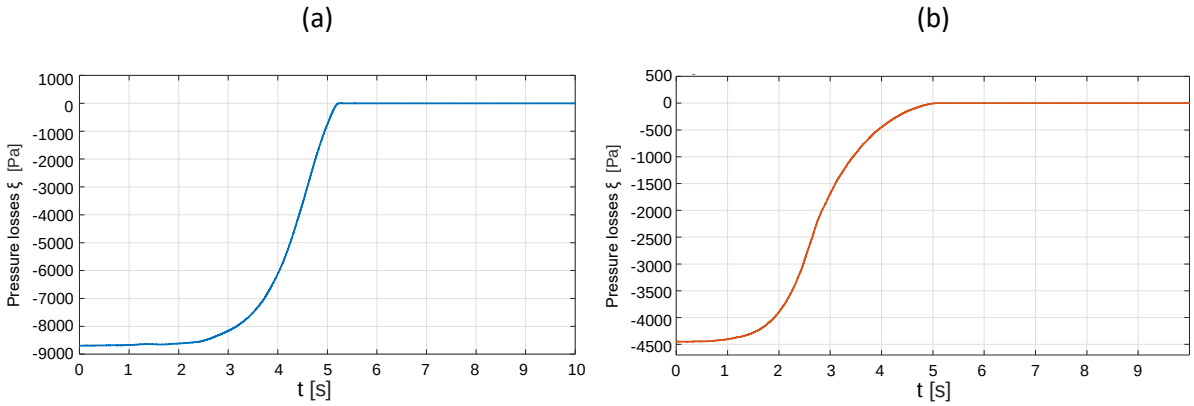

Figure 5-8: Calculated relative pressure losses for test case 1 (a) and test case 2 (b).

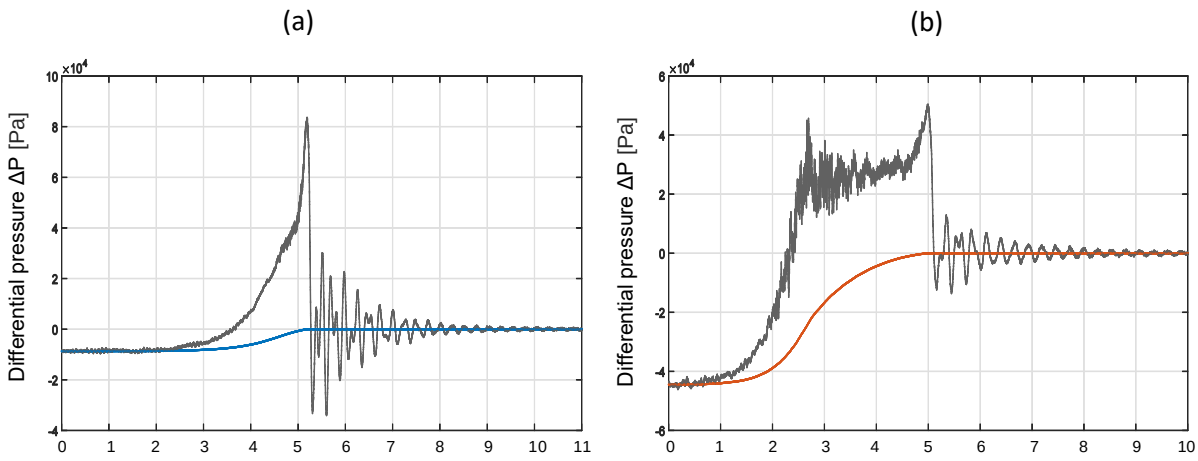

Figure 5-9: Relative differential pressures with the associated calculated pressures losses for test case 1 (a) and test case 2 (b).

The mean values of the flows were calculated to $0.1688\ \mathrm{m}^3/\mathrm{s}$ and $0.3921\ \mathrm{m}^3/\mathrm{s}$, with random errors of $0.33\ \%$ and $0.28\ \%$, respectively. When comparing with the reference flow, the flow at part load given in Figure 5-10 shows a maximum discharge error of approximately $3.32\ \%$. The maximum error of the flow at full load is slightly lower and is located close to $2.74\ \%$. Both relative pressure-time flows are underestimated when applying the computed value of k_1. Still, they are located fairly close to the flows provided by the electromagnetic flowmeter.

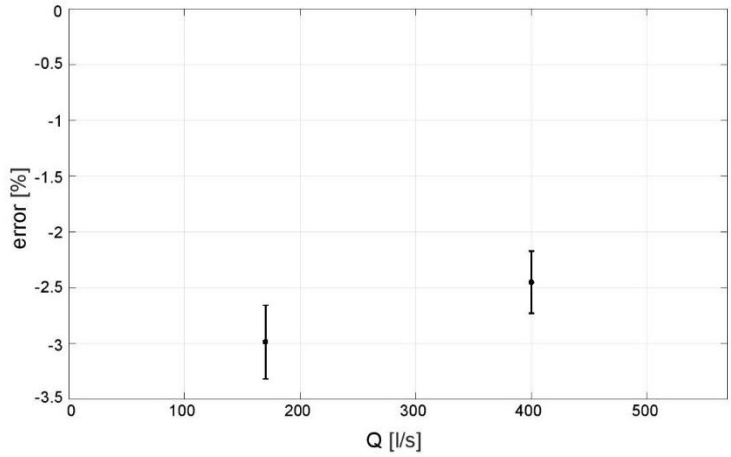

Figure 5-10: Discharge error of the relative flow when applying the computable k1

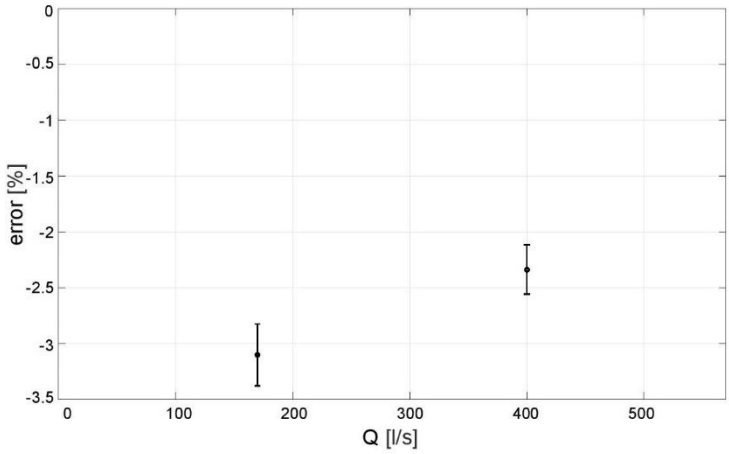

Figure 5-11: Discharge error of the relative flow when removing outliers.

By the removal of two outliers in both test cases, the random errors are decreased further. The random error of test case 1 decreases to 0.278 %, while the maximum discharge increases to 3.38 %. The random error and discharge error for test case two are both reduced to values of 0.221 % and 2.56 %, respectively. The relative results are summarized in Table 5-5:

Test case:	**1**	**2**
	Original results:	
Pressure-time flow Q_{rel}:	0.1688 m^3/s	0.3921 m^3/s
Random uncertainty f_r:	$\pm$0.000556 m^3/s	$\pm$0.00109 m^3/s
Random error e_r:	0.330 %	0.278 %
Student's t:	2.032	2.021
Maximum discharge error e:	3.32 %	2.74 %
	Removal of outliers:	
Number of removed outliers:	2	2
Pressure-time flow Q_{rel}:	0.1686 m^3/s	0.3926 m^3/s
Random uncertainty f_r:	$\pm$0.000423 m^3/s	$\pm$0.000869 m^3/s
Random error e_r:	0.278 %	0.221 %
Student's t:	2.035	2.024
Maximum discharge error e:	3.38 %	2.56 %

Table 5-5: Relative pressure-time results computed at a 95 % confidence level.

5.2.2 Repeatability of the proposed method

The ratio Q_{400}/Q_{170} was investigated for various values of k_1, ranging from $6.72 \cdot 10^{-7}$ to $9.93 \cdot 10^{-5}$, which corresponds to pipe factors in the range of 10 to 1488. 150 points were examined in the given range using the mean values of the relative flows at part load and full load. When taking the ratio of the flows, the geometrical constants are canceled out from the calculation. The remaining ratio reveals to which extent k_1 has affected the pressure losses, and hence the final flows. The results are plotted in Figure 5-12.

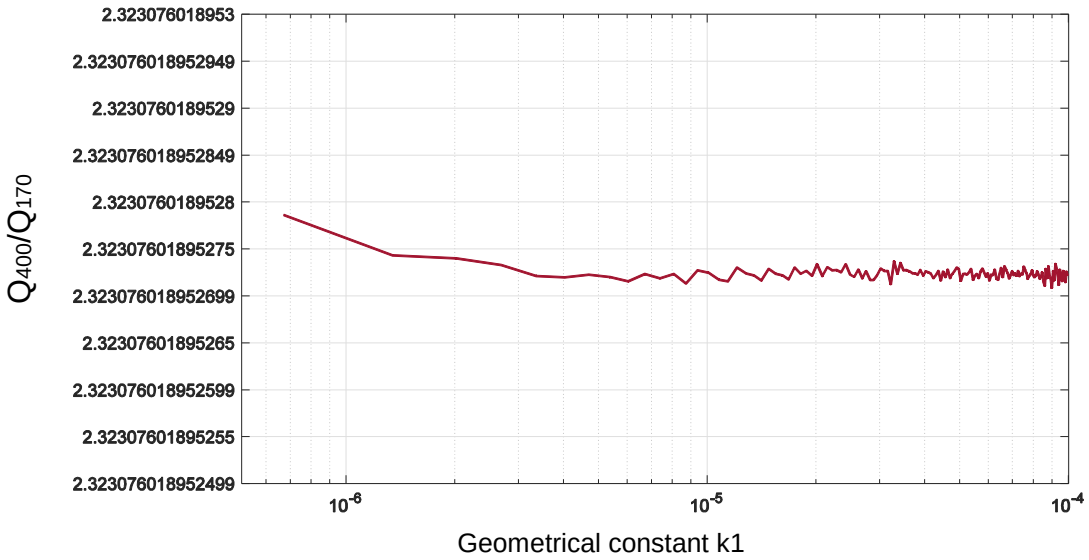

Figure 5-12: The repeatability of the relative measurements for a wide range of geometrical constants on a logaritmic scala.

The ratios show absolutely no sign of inconsistency, implying that the effects caused in the iteration process by k_1 is completely negligible. For the given range, the difference between the minimum and the maximum value is very close to zero. The developed relative pressure-time method succeeds to provide consistency for a wide range of various geometrical constants, regardless of its value. The opposite case would imply a large, unpredictable effect from the constant k_1 or a poor evaluation of the relative pressure-time integral.

The main purpose of applying a relative method is, as previously emphasized, to follow up the decline in performance over time and to examine the improvement after maintenance. Calculating the exact value of the flow rate is not relevant in a relative evaluation. Still, the relative results show that a thorough estimation of k_1 may give an indication of the approximate flow rate. The choice of k_1 has, as stated, a great impact on the final, estimated pressure-time flow. Figure 5-13 presents a case with five integrated pressure-time flows with various geometrical constants:

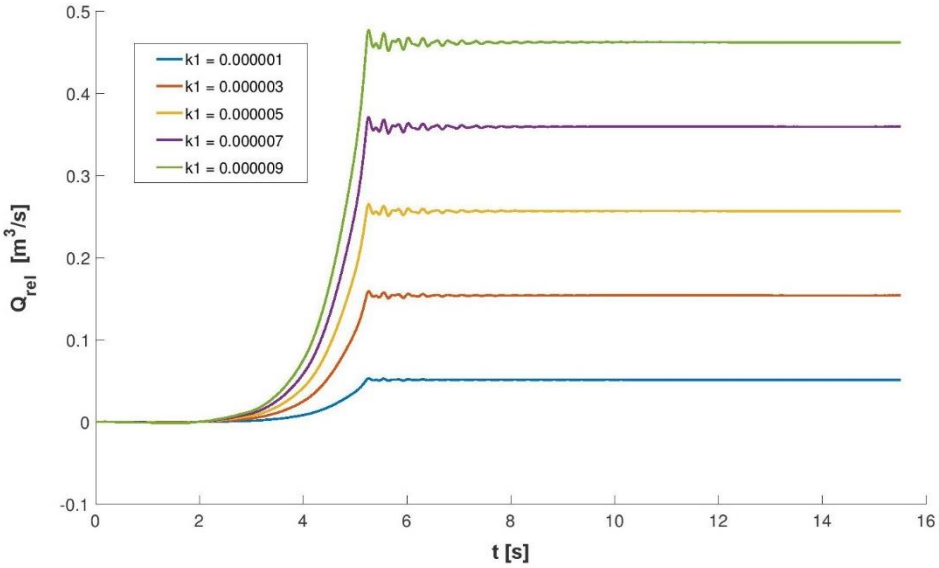

Figure 5-13: Final integrated relative pressure-time flows for various geometrical constants for test case 1.

k_1 ranges from $1 \cdot 10^{-6}$ to $9 \cdot 10^{-6}$, giving final relative flows between $0.05\ m^3/s$ and $0.47\ m^3/s$. The flow is highly dependent on the choice of k_1, which emphasizes the necessity of having a well-computed constant when calculating an estimate of the relative discharge.

The discharge errors of the various methods applied in the pressure-time evaluations are summarized in Figure 5-14 and Figure 5-15. The random errors of the flowmeter flows have also been included.

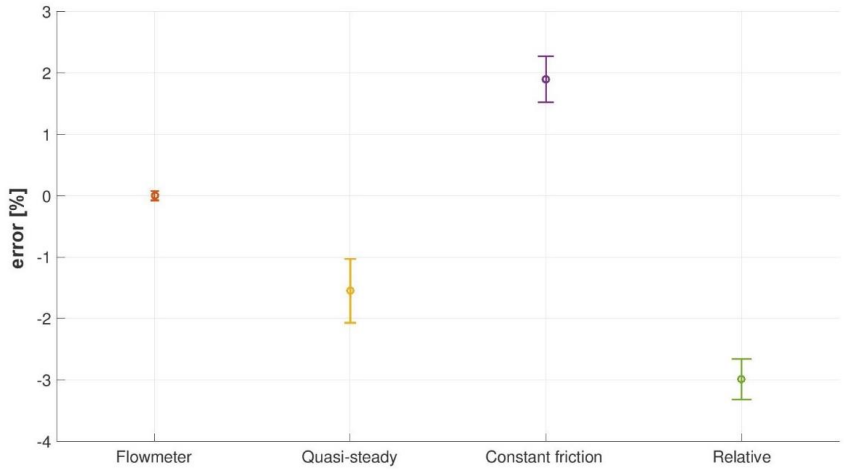

Figure 5-14: A summary of all discharge errors for test case 1. (Original measurements).

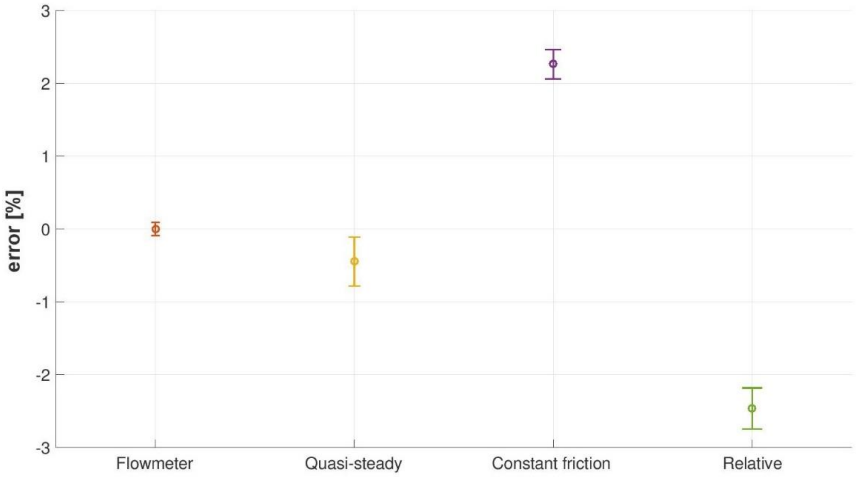

Figure 5-15: A summary of all discharge errors for test case 2. (Original measurements).

Additional figures related to the examination of the relative pressure-time method are attached in *Appendix B.*

6 Numerical results

Two numerical cases were considered to verify the relative pressure-time method, as introduced in section 4.4.1. The developed relative pressure-time method was included in both scripts to provide values of the relative flows. The differential pressures and discharges as a function of time are plotted in Figure 6-1.

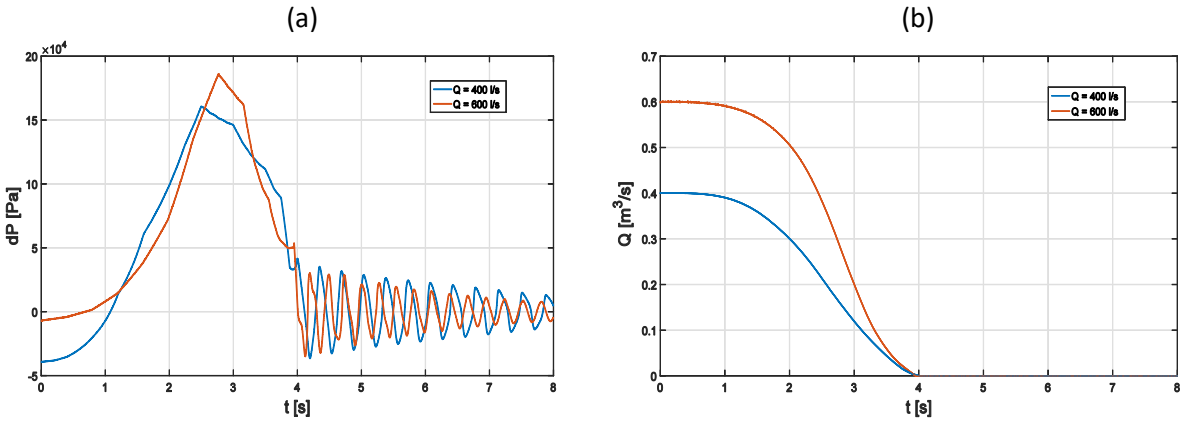

Figure 6-1: (a) Pressure distributions for the simple and complex pipeline. (b) The decrease in discharge during gate closure.

6.1 Computation of the geometrical constants

Two various geometrical constants were considered for pipeline 1 and pipeline 2. Computation of the constants were conducted by application of the pipe factor in Eq. (4.3.2). The geometrical constant for the simple pipeline was calculated to:

$$k_1 = \frac{1}{\rho F} = \ 1.1781 \cdot 10^{-6}$$

Calculation of the corresponding geometrical factor for the complex pipeline was done by accounting for the geometrical variations in the pipeline:

$$k_1 = \frac{1}{\rho F} = \left(\rho\left(\frac{L_1}{A_1} + \frac{L_2}{A_2}\right)\right)^{-1} = 2.0548 \cdot 10^{-6}$$

The reference discharges that were preset in the numerical code, shown in Figure 6-1 (b), are plotted along with the cumulative relative pressure-time integral in Figure 6-2 and Figure

6-2. The final pressure-time flow for the simple pipeline was found equal to $0.4006\ m^3/s$ by taking the average over a wide range of the oscillations after closure.

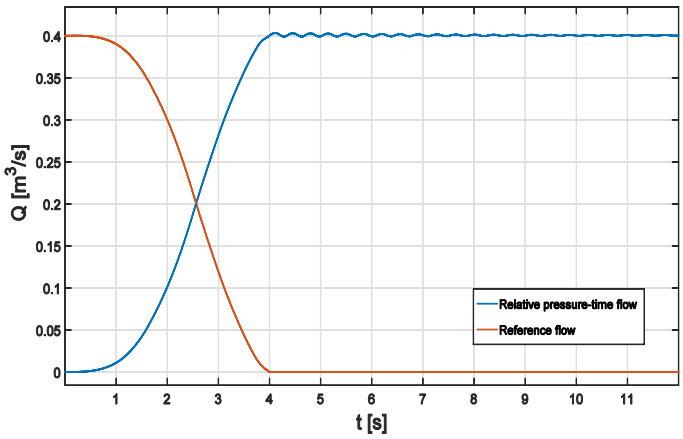

Figure 6-2: The reference flow along with the iterated relative pressure-time flow for the simple pipeline.

The corresponding pressure-time flow for the complex pipeline was calculated to $0.6028\ m^3/s$.

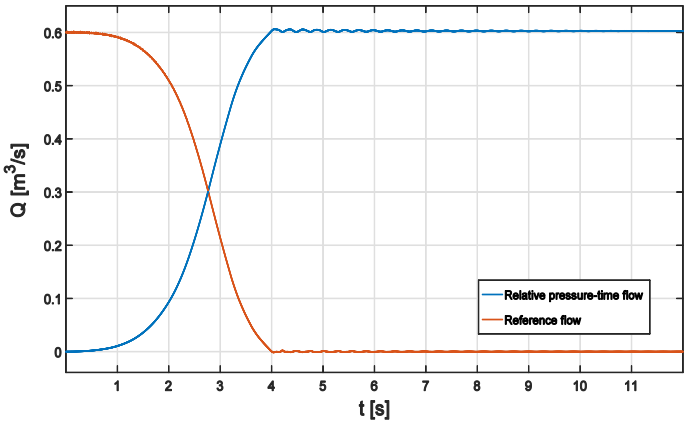

Figure 6-3: The reference flow along with the iterated relative pressure-time flow for the simple pipeline.

The discharge errors of the relative pressure-time flows are plotted in Figure 6-4 by applying Eq. (1.3.7).

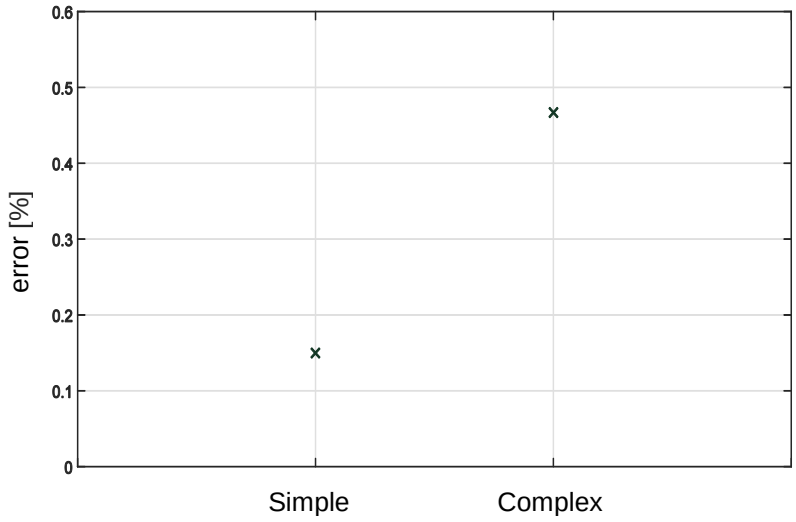

Figure 6-4: Discharge error for the simple and the complex pipeline.

The discharge error of the simple pipeline is $0.15\ \%$, indicating a slightly overestimated flow lying close to the reference flow. The discharge error of the complex pipeline, on the other hand, is considerably larger and has a value close to $0.47\ \%$.

7 Discussion

Absolute pressure-time measurements previously performed in the Waterpower Laboratory at NTNU were applied in the development of a relative pressure-time method. The large number of repetitions in the laboratory experiments enabled a thoroughly and controlled examination of the experimental data by the presented relative procedure. A numerical model was developed in MATLAB to verify the relative results. Two different pipelines were constructed to simulate a valve closure, followed by an implementation of the developed relative procedure. The numerical pressure losses were described by applying both quasi-steady and unsteady friction, as presented in the Brunone friction model. The numerical models were not developed to model the experimental test cases, but to examine the validity of the relative pressure-time method. The results discussed further are entirely based on the measurements where outliers have been removed.

7.1 Experimental results

Although the absolute pressure-time measurements were carried out outside the IEC 41 (1991) standard, both presented friction models managed to provide reasonable estimates of the flows. The discharge error of test case 2 using the quasi-steady method was found approximately equal 0.6 %, which lies within the expected range of uncertainties, given that the pressure-time method is carried out according to the required terms.

The largest discharge error was found in test case 2 when using the constant friction method. It is difficult to state exactly why the discharge error is larger for the flow at full load, but one answer may be that the method's accuracy is poor. The random errors, however, appear lower for test case 2 than for test case 1, as expected. Moreover, the precision of the results tends to be considerably better for the constant friction approach than for the quasi-steady.

One of the major benefits of using relative methods is, as previously stated, that the systematic errors do not affect the measurements. The random errors of both methods are small, with values of approximately 0.28 % and 0.22 % for test case 1 and 2. The repeatability of the measurements is good and the ability of obtaining accurate results appears to be possible by the presented relative method. A simplified approximation to the geometrical constant was conducted, and despite neglecting parts of the bends in the calculation, the method succeeded to provide flows close to the reference flow.

Greater random errors were found in the absolute measurements than in the relative, likely due to the substantial amount of noises in the differential pressure signals. A reduced amount of noise was achieved by conducting a rapid closure to withstand the heavy and

rapid effects by the pressure rise upstream the valve. Only a small amount of noise was present in the relative pressure distribution, as only one of the absolute pressure sensors was applied in the relative analysis. This enables the possibility of having a slow and linear closure when conducting relative measurements in low-head machines with high flow rates.

7.2 Numerical results

The numerical discharge errors were found equal to 0.15 % and 0.47 %, which is fairly close to the reference values. The discrepancy was more considerable for the complex flow, possibly due to some faulty in the numerical code. One of the major challenges was to define the flow coefficients for both cases, which affected the differential pressures and discharges to some extent. An additional assessment of the valve characteristics would have been appropriate for a more thorough numerical assessment. It would also have been expedient to perform the numerical simulations for various flows using equivalent test cases, as it is difficult to state whether the increase in discharge error is caused by a programming error or by the complexity of the pipe. Still, the numerical results encourage the validity of the method, considering that the errors are small when applying the true geometrical constants.

7.3 Relative pressure-time as an alternative

Problems regarding the Winter-Kennedy method were briefly discussed in the introduction. Small changes in the flow pattern, due to i.e. refurbishment or replacement of a turbine, have proved to cause inconsistency between the flow measurements. Various operational conditions, challenges related to calibration of the k constant and old pressure taps have also been designated as sources of the discrepancies (Cervantes et al., 2012).

It is difficult to state to which extent the relative method presented in this thesis may be a better option to the frequently used Winter-Kennedy method, but the main problems related to the Winter-Kennedy are not relevant in the relative pressure-time method. Only one pressure sensor is required in order to conduct the measurements and must be placed upstream a closing device, such as the guide vanes. Furthermore, pressure taps are usually found in the inlet of spiral casings as previously mentioned, enabling a fast and simple implementation of the method. The relative pressure-time method is highly cost-effective as it requires little downtime and equipment to be executed.

While the Winter-Kennedy appears to be highly sensitive to small flow variations in the spiral casing, the relative pressure-time method should work regardless of the flow patterns, as it only considers the differential pressure between a sensor and the reservoir. However, the relative pressure-time method is highly dependent on a good estimate of the viscous losses and a reasonable approach to the geometrical constant. The geometrical constant should remain constant regardless of any maintenance in a hydropower plant seen in a long time perspective. This means that the relative pressure-time measurements may be expected to be consistent for repeated tests, which may prove to simplify the use of relative methods.

8 Conclusion

The main task of this thesis was to develop the standard pressure-time method as a relative method. A relative calculation procedure has been suggested and carried out experimentally and numerically. The method succeeds to obtain repeatable pressure-time flows using a pre-calculated geometrical constant in a relative integration process.

An approximation of the pipe factor for a rather complex pipeline has proved to give a good indication of the flow registered by the electromagnetic flowmeter. Moreover, no inconsistency is detected when calculating of the ratio between the presented flows for a wide range of geometrical constants.

Low-head power plants are in need of a better option to the Winter-Kennedy method and the relative pressure-time alternative presented in this thesis could be a part of the solution. A further verification of the method should be conducted to reveal potential flaws in the presented procedure.

8.1 Further work

The proposed calculation of relative pressure-time method provides promising experimental results and it would be appropriate to conduct field measurements for a further investigation of the method's applicability. This may for instance be done by comparison with the Winter-Kennedy or by an absolute method to detect potential disagreements.

It would also be appropriate to conduct a more thorough investigation of the geometrical constant of the laboratory pipeline. This should be done by including the all bend geometries to examine to which extent they contribute to an improved value.

9 References

ADAMKOWSKI, A. 2012. Discharge Measurement Techniques in Hydropower Systems with Emphasis on the Pressure-Time Method. *In:* SAMADI-BOROUJENI, H. (ed.) *Hydropower - Practice and Application.* InTech.

ADAMKOWSKI, A. & JANICKI, W. 2010. Selected problems in calculation procedures for the Gibson discharge measurement method. *IGHEM.* Rookie, India.

ADAMKOWSKI, A. & JANICKI, W. 2013. A new approach to calculate the flow rate in the pressure-time method - application of the method of characteristics. *HYDRO.* Innsbruck, Austria.

ADAMKOWSKI, A., KRZEMIANOWSKI, Z. & JANICKI, W. 2008. Flow Rate Measurement using the Pressure-Time Method in a Hydropower Plant Curved Penstock. *IGHEM.* Milan, Italy.

ANDERSSON, U., LÖVGREN, M. & ANDRÉE, G. 2008. Skew inlet flow in a model turbine, effects on Winter-Kennedy measurements. *Hydro.* Ljubljana, Slovenia.

ASME PTC 18-2011 2011. Hydraulic Turbines and Pump-Turbines - Performance Test Codes. *Pressure-Time Method.* New York, United States: The Americal Society of Mechanical Engineers.

BERGANT, A., ROSS SIMPSON, A. & VÌTKOVSK, J. 2001. Developments in unsteady pipe flow friction modelling. *Journal of Hydraulic Research,* 39**,** 249-257.

BREKKE, H. 2001. *Hydraulic turbines - Design, erection and operation,* Trondheim, Norway, NTNU.

BRUNONE, B., GOLIA, U. M. & GRECO, M. 1991. Some Remarks on the Momentum Equations for Fast Transients. *International Meeting on Hydraulic Transients with Column Separation, 9th Round Table, IAHR.* Valencia, Spain.

ÇENGEL, Y. A. & CIMBALA, J. M. 2006. *Fluid Mechanics - Fundamentals and Applications,* United States, McGraw-Hill.

CERVANTES, M., ANDRÉE, G., KLASON, P. & SUNDSTRÖM, J. 2012. Flow Measurements in Low-Head Hydro Power Plants. Sweden: Elforsk report.

DAHL, H. 2016. *Development of the Pressure-Time Method.* Project work, NTNU.

DUNCA, G., BUCUR, D. M., CERVANTES, M. J., PROULX, G. & DOSTIE, M. B. 2013. Investigation of the pressure-time method with an unsteady friction. *HYDRO* Innsbruck, Austria.

DUNCA, G., IOVĂNEL, R. G., BUCUR, D. M. & CERVANTES, M. J. 2016. On the Use of the Water Hammer Equations with Time Dependent Friction during a Valve Closure, for Discharge Estimation. *Journal of Applied Fluid Mechanics,* 9**,** 2427-2434.

GIBSON, N. R. 1923. The Gibson method and apparatus for measuring the flow of water in closed conduits. *ASME Power Division*.

IEC 41 1991a. International standard - Field acceptance tests to determine the hydraulic performance of hydraulic turbines, storage pumps and pump-turbines. *Methods of measurement.* Geneva, Switzerland International Electrotechnical Commission.

IEC 41 1991b. International standard - Field acceptance tests to determine the hydraulic performance of hydraulic turbines, storage pumps and pump-turbines. *Appendix C: Analysis of the random uncertainties for a test at constant operating conditions.* Geneva, Switzerland International Electrotechnical Commission.

IEC 41 1991c. International standard - Field acceptance tests to determine the hydraulic performance of hydraulic turbines, storage pumps and pump-turbines. *Table CII: Values of Student's t.* Geneva, Switzerland International Electrotechnical Commission.

JONSSON, P. & CERVANTES, M. 2013. Development of the pressure-time method as a relative and absolute method for low-head hydraulic machines. *Elforsk report*.

JONSSON, P. P. 2011. *Flow and Pressure Measurements in Low-Head Hydraulic Turbines.* Doctoral Thesis, Luleå University of Technology.

JONSSON, P. P., RAMDAL, J., CERVANTES, M. J. & NIELSEN, T. K. 2012. Implementing Unsteady Friction in Pressure-Time Measurements. *IGHEM.* Trondheim, Norway.

LÜDECKE, H.-J. & KOTHE, B. 2006. Water Hammer, KSB Know-how. 1. Available: https://www.ksb.com/blob/7228/b03ed4dd6aa0139a876090d66fe3b9f2/dow-know-how1-water-hammer-data.pdf.

NICOLLE, J. & PROULX, G. 2010. A new method for continuous efficiency measurement for hydraulic turbines. *IGHEM.* Roorkee, India.

NIELSEN, T. K. 05-02-2015 2015. *RE: Efficiency measurements in the field", lecture document, "TEP4200 - Mechanical Design, Operation and Maintenance of Hydraulic Machinery*

SUBRAMANYA, K. 2013. Elements of Hydroelectric Power Engineering - Classification. *Hydraulic Machines.* New Delhi, India: Tata McGraw Hill Education Private Limited.

TULLIS, J. P. 1989. *Hydraulics of Pipelines: Pumps, Valves, Cavitation, Transients,* New York, John Wiley & Sons Inc.

VARDY, A. E. & BROWN, J. M. 1996. On Turbulent, Unsteady, Smooth-Pipe Friction. *Pressure Surges and Fluid Transients***,** 289-311.

WYLIE, E. B. & STREETER, V. L. 1993. *Fluid Transients in Systems,* Englewood Cliffs, New Jersey, US, Prentice-Hall, Inc.

Appendix A: Experimental MATLAB script

The following MATLAB script presents the procedure of evaluating the absolute and relative pressure-time data. The script was initially written for the flow at $0.170\ m^3/s$, but the procedure applies to both flows discussed in this thesis.

```
% %_____________________________________________________________________________________
% %_____________________________ PREPARATION OF DATA_____________________________________
% Preparation part written by ph.D. Joel Sundström from LTU in Sweden

load('Measurement2_thursday_20160428.mat');

flow_ = 0.12433226*data(:,1)-0.24877139;
abs_pipe = (-125.27191713+62.512896*data(:,10))*1000;
abs_pipe2 = (-224.19731877+62.562095*data(:,11)+99.2)*1000;
gate = (285.8763+data(:,9)*-88.26);
Temp = data(:,5)*36-30;
trigger = data(:,17)-2;
t = [0:1/2000:(length(trigger)-1)/2000];
index = find(diff(sign(trigger))==2);
index_dec = index(1:2:end);
index_acc = index(2:2:end);
s = length(index_dec);


for j = 1:s
    dp_dec(:,j) = abs_pipe2(index_dec(j):index_dec(j)+30000)-
abs_pipe(index_dec(j):index_dec(j)+30000);
    p_abs2_dec(:,j) = abs_pipe2(index_dec(j):index_dec(j)+30000);
    p_abs1_dec(:,j) = abs_pipe(index_dec(j):index_dec(j)+30000);
    t_dec(:,j) = t(index_dec(j):index_dec(j)+30000);
    temp_dec(:,j) = Temp(index_dec(j):index_dec(j)+30000);
end

for j = 1:s
    dp_acc(:,j) = abs_pipe2(index_acc(j):index_acc(j)+30000)-
abs_pipe(index_acc(j):index_acc(j)+30000);
end

for j = 1:s
    gate_dec(:,j) = gate(index_dec(j):index_dec(j)+30000);
    flow_dec(:,j) = flow_(index_dec(j):index_dec(j)+30000);
end

for j = 1:s
    gate_dec2(:,j) = smooth(gate_dec(:,j),50);
end

for j = 1:s
    index_temp = find(gate_dec2(2000:3000,j)<99.7);
    index_dec2(j) = index_temp(1)+2000;
```

```
end

dp_dec = [];
p_abs2_dec = [];
p_abs1_dec = [];
t_dec = [];
temp_dec = [];
gate_dec = [];


for j = 1:s
    dp_dec(:,j) = abs_pipe2(index_dec(j)+index_dec2(j)-1000:index_dec(j)+index_dec2(j)+30000)-
abs_pipe(index_dec(j)+index_dec2(j)-1000:index_dec(j)+index_dec2(j)+30000);
    p_abs2_dec(:,j) = abs_pipe2(index_dec(j)+index_dec2(j)-
1000:index_dec(j)+index_dec2(j)+30000);
    p_abs1_dec(:,j) = abs_pipe(index_dec(j)+index_dec2(j)-
1000:index_dec(j)+index_dec2(j)+30000);
    t_dec(:,j) = t(index_dec(j)+index_dec2(j)-1000:index_dec(j)+index_dec2(j)+30000);
    temp_dec(:,j) = Temp(index_dec(j)+index_dec2(j)-1000:index_dec(j)+index_dec2(j)+30000);
    gate_dec(:,j) = gate(index_dec(j)+index_dec2(j)-1000:index_dec(j)+index_dec2(j)+30000);
end


v = [1 5:18 20:22 24:32 36 38:46 49];
index_dec = index_dec(v);
s = length(index_dec);
index_dec2 = index_dec2(v);

dp_dec = [];
p_abs2_dec = [];
p_abs1_dec = [];
t_dec = [];
temp_dec = [];
gate_dec = [];
flow_dec = [];

for j = 1:s
    dp_dec(:,j) = abs_pipe2(index_dec(j)+index_dec2(j)-1000:index_dec(j)+index_dec2(j)+30000)-
abs_pipe(index_dec(j)+index_dec2(j)-1000:index_dec(j)+index_dec2(j)+30000);
    p_abs2_dec(:,j) = abs_pipe2(index_dec(j)+index_dec2(j)-
1000:index_dec(j)+index_dec2(j)+30000);
    p_abs1_dec(:,j) = abs_pipe(index_dec(j)+index_dec2(j)-
1000:index_dec(j)+index_dec2(j)+30000);
    t_dec(:,j) = t(index_dec(j)+index_dec2(j)-1000:index_dec(j)+index_dec2(j)+30000);
    temp_dec(:,j) = Temp(index_dec(j)+index_dec2(j)-1000:index_dec(j)+index_dec2(j)+30000);
    gate_dec(:,j) = gate(index_dec(j)+index_dec2(j)-1000:index_dec(j)+index_dec2(j)+30000);
    flow_dec(:,j) = flow_(index_dec(j)+index_dec2(j)-1000:index_dec(j)+index_dec2(j)+30000);
end


for j = 1:s
    temp(j ) = mean(dp_dec(end-10000:end,j));
    dp_dec(:,j) = dp_dec(:,j)-temp(j);
end
```

```
% %_____________________________ ABSOLUTE ANALYSIS_____________________________


Fs = 2000; % Sample frequency
rho = 999; % Density of water
L = 4; % Length of measuring section
Ag = pi*0.3^2*0.25; % Cross-sectional area of measuring section
R = 0.15; % Radius of pipe
t = [0:1/Fs:(length(dp_dec(:,1))-1)/Fs]; % Time scale of measurements
k = Ag/rho/L; % Geometrical constant in front of PT integral
g = 9.81; % Gravitational constant
colebr = @colebrook; % Function calculating the Colebrook friction factor

% %_____________________________________________________________________________
% Adjusting dP_dec to static line end:
mval_ = zeros(1,s); % s = number of measurements

for i = 1:s
        mval_(i) = mean(mean(dp_dec(22000:end,i)));
end
for j = 1:s
    for i = 1:31001
            dp_dec(i,j) = (dp_dec(i,j)-mval_(j));
    end
end


% %_____________________________________________________________________________
% Initial flow "losses", assuming linear loss:
losses=zeros(31001,1); % For Q = 170 l/s

for i = 1:4179
    losses(i,1) = mean(mean(dp_dec(1:913,1)));
end

x = 0;
for i = 4180:10450
    losses(i,1) = 0.081172635943*x-509.0336;
    x = x+1;
end

for i = 10451:31001
    losses(i,1) = 0;
end


% %_____________________________________________________________________________
% Mean initial values of the pressures from absolute sensors 1 and 2:
P1_abs = zeros(1,s);
P2_abs = zeros(1,s);

for i = 1:s
    P1_abs(i) = mean(mean(p_abs1_dec(1:600,i)));
    P2_abs(i) = mean(mean(p_abs2_dec(1:600,i)));
end
```

```
% %_____________________________________________________________________________________________
% %_____________________________________ELECTROMAGNETIC FLOWMETER_____________________________
% % Mean values from the flowmeter:
zline = zeros(31001,s);

for j = 1:s
    zline(1:31001,j) = mean(flow_dec(1:950,j));
end


% %_____________________________________________________________________________________________
% %_____________________________________________________________________________________________
% Absolute pressure-time measurements with linear pressure loss.
% Finding initial flows for quasi-steady:
Q_1 = zeros(1,s);
Q_1_ = zeros(1,s);
Q_init = zeros(31001,s);

for j = 1:s
    Q_1Q = k*trapz(t,dp_dec(:,j)-losses); % Initial values of Q
    Q_1(j) = Q_1Q;

    Q_1_Q = k*trapz(t,dp_dec(:,j)-losses); % Initial values of Q
    Q_1_(j) = Q_1_Q;

    Q_initQ = k*cumtrapz(t,dp_dec(:,j)-losses); % Initial culumative integral of Q
    Q_init(:,j) = Q_initQ;
end


QI = zeros(1,s);

%Fixed value of initial flow QI:
for j = 1:s
    QI(1,j) = Q_1(1,j);
end

% Absolute pressure losses:
PL_abs = zeros(1,s);

for i = 1:s
    PL_abs(i) = (P1_abs(i)-P2_abs(i)); % Pressure loss in measuring section
end


% %_____________________________________________________________________________________________
% %_____________________________________CONSTANT FRICTION_____________________________________


visc = 0.0000011092; % Viscosity of fluid
e = 0.000015; % Roughness
K_rou = e/0.3; % Roughness/diameter

Q_1c = k*trapz(t,dp_dec(:,1)-losses);
```

```
% Initial flow for constant friction:
Q_init_mat = zeros(31001,s);
Q_1c_ = zeros(1,s);

for j = 1:s
        Q_initc = k*cumtrapz(t,dp_dec(:,j)-losses);
        Q_init_mat(:,j) = Q_initc;
        Q_1c_mat = k*trapz(t,dp_dec(:,j)-losses);
        Q_1c_(:,j) = Q_1c_mat;
end

% Initial cumulative reynolds numbers:
Re = zeros(31001,s);

for j = 1:s
    for i = 1:31001
        Re(i,j) = (((Q_init_mat(i,j)./Ag).*0.3)./visc);%((Q_1_qs/Ag)*0.3)/visc;
    end
end

Re_init = zeros(1,s); % Initial reynolds number of each measurement
f_i = zeros(1,s); % Initial friction of each measurement

for j = 1:s
    Re_init(j) = mean(mean(Re(17700:end,j)));

        if Re_init(j) < 0
            f_i(j) = 0;
        elseif Re_init(j) == 0
            f_i(j) = 0;
        elseif Re_init(j) < 2300
            f_i(j) = 64/Re_init(j);
        else
            f_i(j) = colebr(Re_init(j),K_rou);
        end
end

% Tolerance of convergence:
tol = 1*10^-14;

% Initalization of final PT matrix:
Q_ctc_mat = zeros(31001,s);

% PT with constant friction
for j = 1:s

    i = 1;
    Q_1c = Q_1c_(1,j);
    Q_ctc = Q_1c;
    Q_res = Q_ctc;

    while Q_res > tol

        Q_ctc = k*cumtrapz(t,dp_dec(:,j)-((f_i(1,j)*L*rho)/(0.3*2*(Ag^2))).*(Q_ctc-
Q_1c).*abs(Q_ctc-Q_1c)); % Cumulative integral
        Q_c = mean(mean(Q_ctc(15000:end))); % Final value of Q
```

```
        Re_fric = ((Q_c/Ag)*0.3)/visc; % Calculating new value of Re
        if Re_fric < 0
            f_i(1,j) = 0;
        elseif Re_fric == 0
            f_i(1,j) = 0;
        elseif Re_fric < 2300
            f_i(1,j) = 64/Re_fric;
        else
            f_i(1,j) = colebr(Re_fric,K_rou);
        end

        Q_res = abs(Q_c-Q_1c);
        Q_1c = Q_c; % Initializing new value of Q_1
        i = i+1; % Iterating until Q_residual is satisfied
    end

    Q_ctc_mat(:,j) = Q_ctc; % PT matrix containing cumulative integrals of all measurements
end
hold off


% %_____________________________________________________________________________________
% %_____________________________ QUASI-STEADY FRICTION_____________________________________


% Initial value of Q:
Q_ct_Q = zeros(1,s);

for j = 1:s
    Q_ct_Q(1,j) = QI(1,j);
end

% Initalization of final PT matrix:
Q_ct_mat = zeros(31001,s);

% PT with quasi-steady friction
for j = 1:s

    Q_ct_ = Q_ct_Q(1,j);
    Q_residual = Q_ct_;
    i = 1;

    while Q_residual > tol

        Q_ct_ = k*cumtrapz(t,dp_dec(:,j)-((PL_abs(1,j)/(Q_1_(1,j)*abs(Q_1_(1,j)))).*(Q_ct_-
Q_1_(1,j)).*abs(Q_ct_-Q_1_(1,j))));
        Q_q(i) = mean(mean(Q_ct_(15000:end)));
        Q_residual = abs(Q_q(i)-Q_1_(1,j));
        Q_1_(1,j) = Q_q(i); % Initializing new value of Q_1
        i = i+1; % Iterating until Q_residual is satisfied
    end

    Q_ct_mat(:,j) = Q_ct_;

end
```

```
% %_____________________________________________________________________________
% %_____________________________ RELATIVE ANALYSIS ____________________________________


p_atm = 98150; % Initial pressure loss:
P1_i = p_atm; % Pressure at reservoir
P2_i = mean(mean(p_abs2_dec(1:100,:))); % Pressure at pressure sensor 2
Qi = mean(flow_dec(1,:)); % Mean flow from flowmeter


% %_____________________________ INITIAL PRESSURE LOSS ____________________________________

% % Calculating the pressure loss:
dp = zeros(31001,s);

for j = 1:s
    for i = 1:31001;
        dp(i,j) = (p_abs2_dec(i,j)-p_atm);
    end
end

% % Adjusting the differential pressures to the static line end
mval = zeros(1,s);
dp_ = zeros(31001,s);

for i = 1:s
        mval(i) = mean(mean(dp(25000:end,i)));
end

for j = 1:s
    for i = 1:31001
            dp_(i,j) = (p_abs2_dec(i,j)-p_atm)-mval(j);
    end
end


% % Individual initial pressure lossses from each measurement
PL_i = zeros(1,s);

for i = 1:s
    PL_i(i) = -(mean(dp_(1:600,i)));
end


% Initial pressure loss, assuming linear loss:
loss = zeros(31001,1); % For Q = 170 l/s

for i = 1:3543
    loss(i,1) = mean(mean(dp_(1:913,1)));
end

x = 0;
for i = 3544:10450
    loss(i,1) = 1.29435274*x-8906.9;
    x = x+1;
end
```

```
for i = 10451:31001
    loss(i,1) = 0;
end



% %_____________________________ INITIAL VALUES _____________________________________________

% Geometrical factor k1:
k1 = 0.0000032993; % Computational


% Initial relative flow, assuming linear losses:
Q_rel = zeros(31001,s);
Q_1r = zeros(1,s);
Q_1rel = zeros(1,s);
Q_1rel_qs = zeros(1,s);

for i = 1:s
    Q_rel_temp=k1*cumtrapz(t,dp_(:,i)-loss); % Initial, relative flow
    Q_rel(:,i) = Q_rel_temp;

    Q_1r_temp = k1*trapz(t,dp_(:,i)-loss); % Initial, relative flow
    Q_1r(1,i) = Q_1r_temp;

    Q_1rel(1,i) = Q_1r_temp;
    Q_1rel_qs(1,i) = Q_1r_temp;
end


% %_____________________________________________________________________________________________
% %_____________________________________RELATIVE PRESSURE-TIME_____________________________________

%Fixed value of initial flow QIr:
QIr = zeros(1,s);

for i = 1:s
    QIr(i) = Q_1rel(1,i);
end

% Initialization of final PT matrix
Q_relative_mat = zeros(31001,s);

for j = 1:s

    i = 1;
    Q_ctr = QIr(1,j);
    Q_residual = Q_ctr;

    while Q_residual > tol

          Q_ctr = k1*cumtrapz(t,dp_(:,j)-((PL_i(1,j)/(Q_1rel(1,j)*abs(Q_1rel(1,j)))).*(Q_ctr-
Q_1rel(1,j)).*abs(Q_ctr-Q_1rel(1,j))));
          Q_r(i) = mean(mean(Q_ctr(15000:end)));
          Q_residual = abs(Q_r(i)-Q_1rel(1,j));
          Q_1rel(1,j) = Q_r(i); % Initializing new value of Q_1r
          i = i+1; % Iterating until Q_residual is satisfied
```

```
    end

    Q_relative_mat(:,j) = Q_ctr; % Relative PT matrix for relative measurements
end




% % ____________________________________________________________________________________
% % ________________________STATISTICAL ANALYSIS:_____________________________________


t_dist = @student_t_distribution; % Student's t from separate function

% Final mean flows for all methods - Taking the mean over oscillations:
Q_abs_mva = zeros(1,s);
Q_flow_mval = zeros(1,s);
Q_quasisteady1 = zeros(1,s);
Q_matr_meanvalue = zeros(1,s);
Q_constantfric = zeros(1,s);


for i = 1:s

        Q_flow_mval(i) = mean(flow_dec(1:850,i)); % Flows from flowmeter
        Q_quasisteady1(i) = mean(Q_ct_mat(18000:end,i)); % Quasi-steady flows
        Q_matr_meanvalue(i) = mean(Q_relative_mat(18000:end,i)); % Relative flows
        Q_constantfric(i) = mean(Q_ctc_mat(18000:end,i)); % Flows from constant friction
end


% randomerror = statistical analysis of chosen measurement,
% i.e. Q_matr_meanvalue:
randomerror = Q_matr_meanvalue;

N = length(randomerror); % Number of independent measurements
V = N-1; % Degree of freedom

Y_mean = mean(randomerror); % Mean value of relative Q
Y_r = randomerror; % Mean array of relative Q



% ESTMIATED STANDARD DEVIATION: (Matlab funvtion: std(Y_r))
S_y = zeros(1,N);

for i = 1:length(Y_r)
    S_y(1,i) = (Y_r(i)-Y_mean)^2;
end

S_Y = sqrt((sum(S_y)/(N-1))); % Estimated standard deviation.
S_Y_m = S_Y/sqrt(N); % Standard deviation of the mean
```

```
% OTHER PARAMETERS:
S_var = var(Y_r);
S_min = min(Y_r);
S_max = max(Y_r);
S_range = range(Y_r);



% t-students distribution:
t_sqrtn = t_dist(V); % Student's t, t/sqrt(n)
tS_Y = t_sqrtn*S_Y;


% Random uncertainty associated with the mean value at the
% 95 % confidence level:
e_r = t_sqrtn*S_Y; % +/- value of random uncertainty
ran_error = (e_r/Y_mean)*100; % [%] %Random error
```

Published with MATLAB® R2015a

Appendix B: Additional figures

Figure B - 1 and Figure B - 2 illustrates the iterative process of determining the final relative pressure-time flows for test case 1 and 2, respectively.

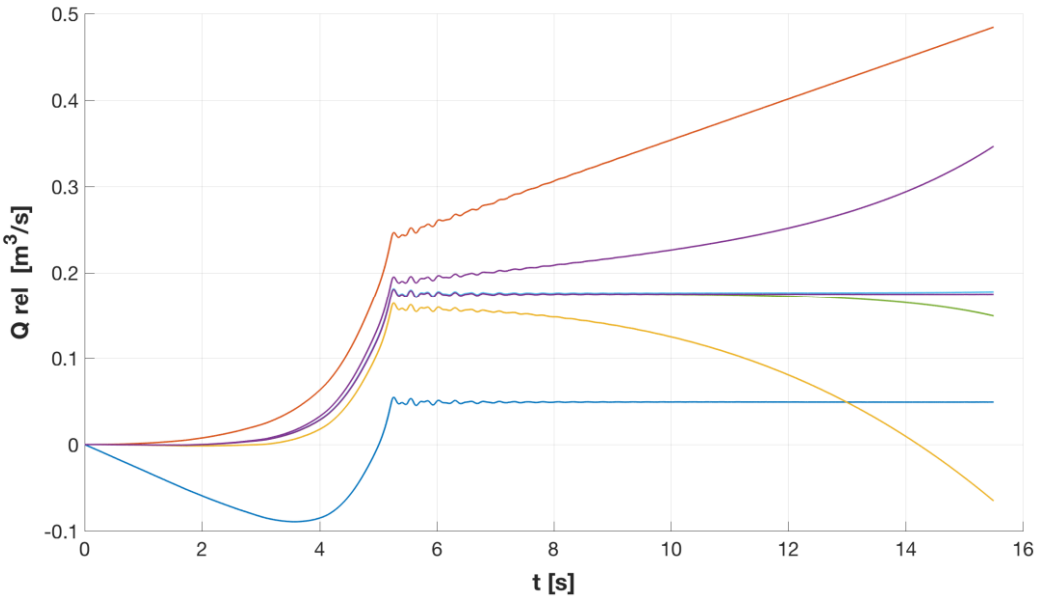

Figure B - 1: Iterative process of the relative measurements for test case 1. Numer of iterations: 23

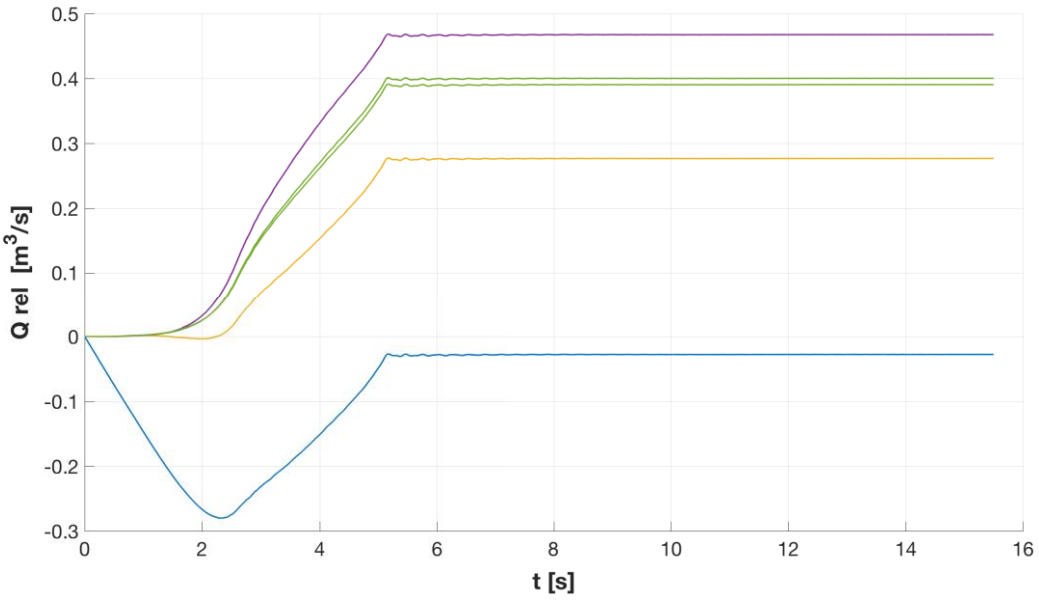

Figure B - 2: Iterative process of the relative measurements for test case 2. Numer of iterations: 26

Figure B - 3 and Figure B - 5 present the approximated cumulative integral of the relative differential pressures. The oscillations in the figures are plotted in Figure B - 4 and Figure B - 6.

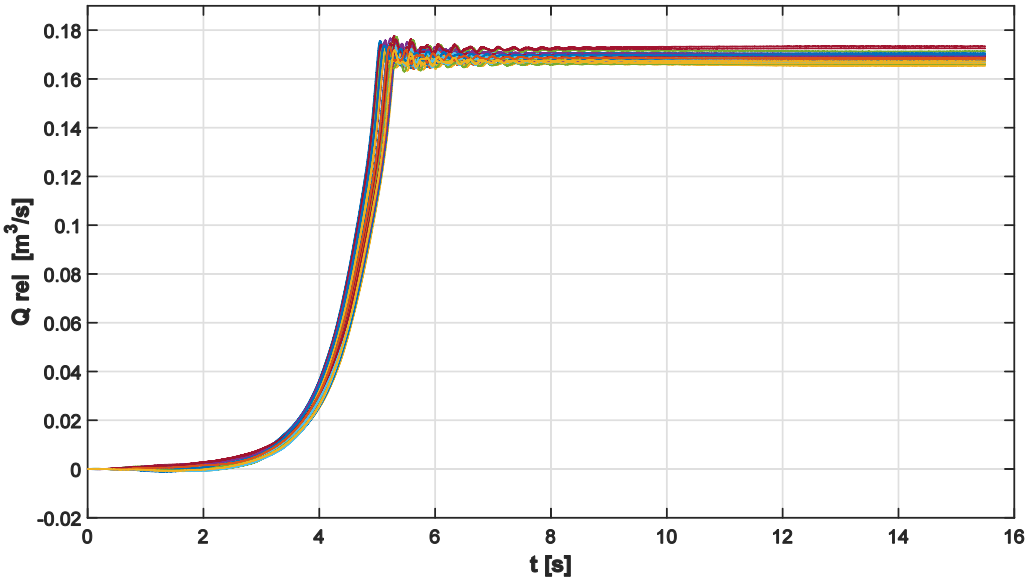

Figure B - 3: Presentation of the cumulative relative pressure-time integral. 38 repetitions carried out on test case 1.

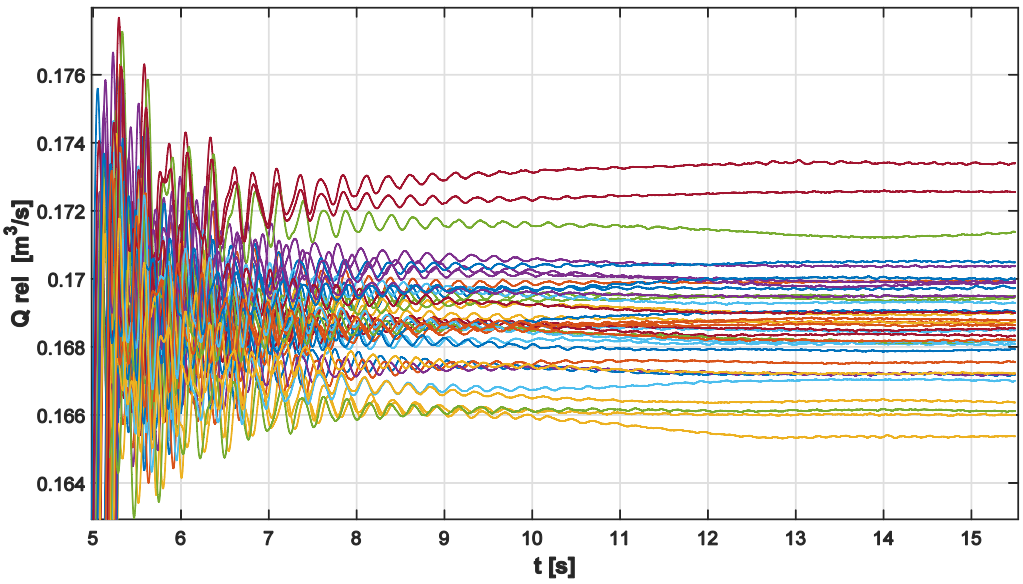

Figure B - 4: A closer inspection of the oscillations in the cumulative pressure-time integral.

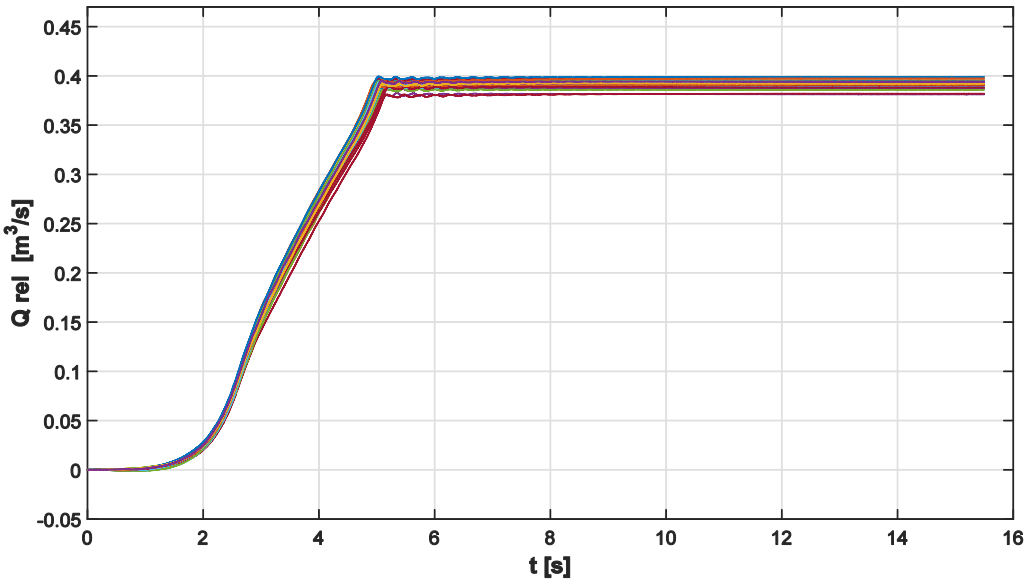

Figure B - 5: Presentation of the cumulative relative pressure-time integral. 46 repetitions carried out on test case 2.

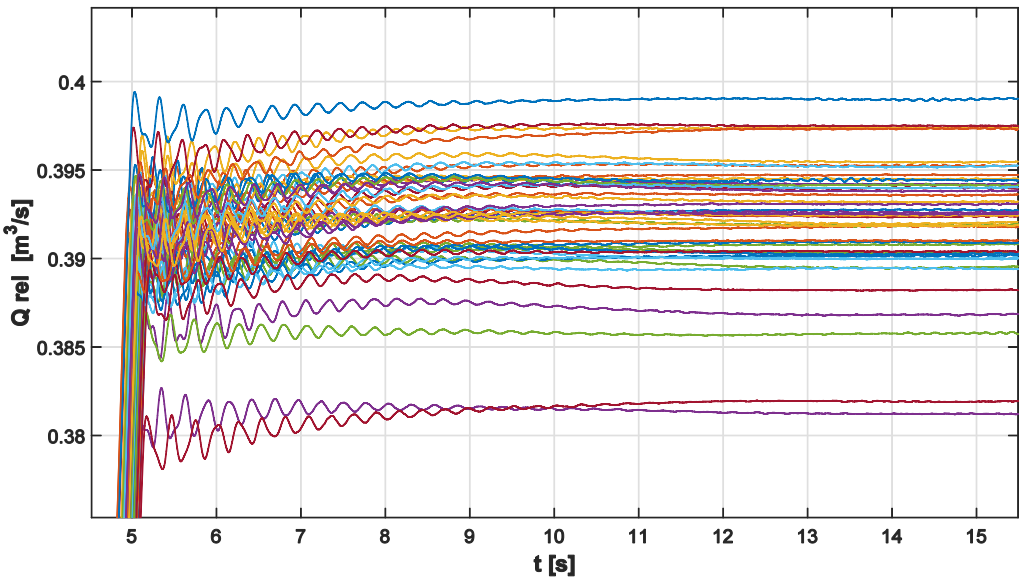

Figure B - 6: A closer inspection of the oscillations in the cumulative pressure-time integral.

Appendix C: Derivation of the characteristic equations

Momentum equation:

$$g\frac{\partial H}{\partial x}+\frac{fV|V|}{2D}+V\frac{\partial V}{\partial x}+\frac{\partial V}{\partial t}=0 \qquad (C-1)$$

Continuity equation:

$$V\frac{\partial H}{\partial x}+\frac{\partial H}{\partial t}+\frac{a^2}{g}\frac{\partial V}{\partial x}=0 \qquad (C-2)$$

The momentum and continuity equations may be simplified by neglecting the advective terms $V\partial V/\partial x$ and $V\partial H/\partial x$. The reduced equations are denoted L_1 and L_2:

$$L_1=g\frac{\partial H}{\partial x}+\frac{fV|V|}{2D}+\frac{\partial V}{\partial t}=0 \qquad (C-3)$$

$$L_2=\frac{\partial H}{\partial t}+\frac{a^2}{g}\frac{\partial V}{\partial x}=0 \qquad (C-4)$$

A linearly relation between L_1 and L_2 is found by multiplying the continuity equation with an unknown constant λ:

$$L=L_1+\lambda L_2 \qquad (C-5)$$

$$L=\left(g\frac{\partial H}{\partial x}+\frac{fV|V|}{2D}+\frac{\partial V}{\partial t}\right)+\lambda\left(\frac{\partial H}{\partial t}+\frac{a^2}{g}\frac{\partial V}{\partial x}\right)=0 \qquad (C-6)$$

Rearranging the expression gives:

$$\lambda\left(\frac{g}{\lambda}\frac{\partial H}{\partial x}+\frac{\partial H}{\partial t}\right)+\left(\frac{a^2}{g}\frac{\partial V}{\partial x}+\frac{\partial V}{\partial t}\right)+\frac{fV|V|}{2D}=0 \qquad (C-7)$$

The total derivatives of $H=f(t,x)$ and $V=f(t,x)$ with respect to t are defined as:

$$\frac{dH}{dt}=\frac{\partial H}{\partial x}\frac{dx}{dt}+\frac{\partial H}{\partial t} \qquad (C-8)$$

$$\frac{dV}{dt}=\frac{\partial V}{\partial x}\frac{dx}{dt}+\frac{\partial V}{\partial t} \qquad (C-9)$$

The values of the constant λ is found by inserting Eq. (C - 8) and Eq. (C - 9) into Eq. (C - 7):

$$\lambda = \pm\frac{g}{a} \qquad \textit{(C - 10)}$$

The final characteristic functions $C^+$and C^- are further derived from Eq. (C - 7) by inserting the positive and negative value of the constant in Eq. (C - 10):

$$C^+\ equation\text{:} \quad \begin{cases} \frac{g}{a}\frac{dH}{dt} + \frac{dV}{dt} + \frac{fV|V|}{2D} = 0 \\ for\ \frac{dx}{dt} = a \end{cases} \qquad \textit{(C - 11)}$$

$$C^-\ equation\text{:} \quad \begin{cases} \frac{g}{a}\frac{dH}{dt} - \frac{dV}{dt} - \frac{fV|V|}{2D} = 0 \\ for\ \frac{dx}{dt} = -a \end{cases} \qquad \textit{(C - 12)}$$

Appendix D: Numerical MATLAB script

The following MATLAB script presents the complex pipe flow with an initial discharge of $0.600\ m^3/s$ using the method of characteristics (MOC).

```
% %_____________________________________________________________________________
% %_____________________________ PREPARATION OF DATA_____________________________


% Functions applied in code:
lin = @linint; % Linear interpolation of flow coefficient
colebr = @colebrook; % Function calculating the Colebrook friction factor

visc = 0.0000011092; % m^2/s, kinematic viscosity
rho = 999; % [kg/m?3], density of water:
e = 0.000015; % Roughness
g = 9.81; % [m/s^2], acceleration of gravity:

% Various pipe diameters:
D1 = 0.5; % Subscript 1 means pipe 1
D2 = 0.3; % Subscript 2 means pipe 2

% Bulk modulus of elasticity:
K1 = 2.15*10^9; % [Pa]
K2 = 2.15*10^9; % [Pa]

E = 180*10^9; %Young modulus
et = 0.002; % Wall thickness

% Wave speed number for pipes:
a1 = 925.9259;%(sqrt(K1/rho))/(sqrt(1+((K1*D1)/(E*et))));
a2 = 925.9259;%(sqrt(K1/rho))/(sqrt(1+((K1*D2)/(E*et))));

% Pipe areas:
A1 = pi*(D1/2)^2;
A2 = pi*(D2/2)^2;

% Length of pipe segments:
L1 = 40;
L2 = 20;

%Roughness of pipe segments (Pipe roughness over pipe diameter):
K_rough1 = e/D1;
K_rough2 = e/D2;

HR1 = 4; % Initial piezometric head[m], reservoir
HR2 = 0; % Head of downstream reservoir

QI = 0.6; % Initial discharge [m3/s]
HI = HR1; % Initial height

t1 = 0;
t = 0; % Time start
```

```
tmax = 12; % [s] Duration of simulation
tc = 4; % Valve closure time

%Pipe nodes:
N1 = 16;
N2 = 8;

NS1 = N1+1; % End of pipe
NS2 = N2+1; % End of pipe

% Length between node sections:
dx1 = L1/N1;
dx2 = L2/N2;

% Time steps:
dt1 = dx1/a1;
dt2 = dx2/a2;

% Decides end of simulation:
nr_t = round(tmax/dt1);

% Pipeline characteristic impedance:
B1 = a1/(g*A1);
B2 = a2/(g*A2);

% Initial valve opening, from 0 - 1 :
VOI = 1;

% Frictional correction value:
corrval = 55;


% %_____________________________________________________________________________
% %_____________________________STEADY STATE:_____________________________________

VI = QI/A1; % Initial bulk velocity
ReI1 = (VI*D1)/visc; % Initial Reynold's number:
    if ReI1 < 2300
        fq1 = 64/ReI1;
    else
        fq1 = colebr(ReI1,K_rough1);
    end

VI = QI/A2; % Initial bulk velocity
ReI2 = (VI*D2)/visc; % Initial Reynold's number:
    if ReI2 < 2300
        fq2 = 64/ReI2;
    else
        fq2 = colebr(ReI2,K_rough2);
    end


% Only quasi-steady friction contributing.
f1 = fq1;
f2 = fq2;

% INITIAL VALUES FOR H AND Q:
H1 = zeros(1,NS1);
```

```
H2 = zeros(1,NS2);
Q1 = zeros(1,NS1);
Q2 = zeros(1,NS2);


    for i = 1:NS1
            Q1(i) = QI;
            H1(i) = HR1-((f1*(QI^2)*((i-1)*dx1))/(2*g*D1*(A1^2)));
    end

    for i = 1:NS2
            H2(i) = H1(NS1)-((f2*(QI^2)*((i-1)*dx2))/(2*g*D2*(A2^2)));
            Q2(i) = QI;
    end

   H2(NS2) = 0;
```

_____SIMULATION START:_____

```
count = 1; % Counts for each time step

Q1_temp = zeros(10,N1+1);
H1_temp = zeros(10,N1+1);
Q2_temp = zeros(10,N2+1);
H2_temp = zeros(10,N2+1);

tol = 1*10^(-14); % Tolerance of convergence

Re1 = zeros(1,NS1);
fq1 = zeros(1,NS1);
J1_pos = zeros(1,NS1);
J1_neg = zeros(1,NS1);

Re2 = zeros(1,NS2);
fq2 = zeros(1,NS2);
J2_pos = zeros(1,NS2);
J2_neg = zeros(1,NS2);

while count~=(nr_t+2)
```

```
%
%_____
_____
```

BOUNDARY CONDITIONS FOR NODE 2 to N. PIPE 1.

```
        for i = 2:N1;

            %First calculating Reynolds number:
            Re1(i) = ((Q1(i)/A1)*D1)/visc;

            %Calculating quasi-steady fq:
            if Re1(i) < 2300
                fq1(i) = 64/Re1(i);
            else
```

```
                fq1(i) = colebr(Re1(i),K_rough1);
            end

            %Then calculating C_star:
            if Re1(i) < 2300
                C_star(i) = 0.00476;
            else
                C_star(i) = 7.41/(Re1(i)^(log(14.3/(Re1(i)^0.05))));
            end

            % Brunone friction coefficient k:
            k(i) = sqrt(C_star(i))/2;
            k(i) = corrval*k(i);

            QP_ = Q1(i); % Temporary value of QP1 = QP_
            Q_residual = tol;

            while Q_residual >=tol
                % Pressure losses from positive characteristic lines:
                J1_pos(i) = (fq1(i)*Q1(i-1)*abs(Q1(i-
1))/(2*g*D1*A1^2))+((k(i)/(2*g*A1))*((QP_-Q1(i))/dt1));
                % Pressure losses from negative characteristic lines:
                J1_neg(i) =
(fq1(i)*Q1(i+1)*abs(Q1(i+1))/(2*g*D1*A1^2))+((k(i)/(2*g*A1))*((QP_-Q1(i))/dt1));

                CP = H1(i-1)+(B1*Q1(i-1))-(J1_pos(i)*dx1);
                CM = H1(i+1)-(B1*Q1(i+1))+(J1_neg(i)*dx1);

                HP1(i) = 0.5*(CP+CM); % HP value for pipe 1
                QP1(i) = (CP-HP1(i))/B1; % QP value for pipe 1

                Q_residual = abs(QP1(i)-QP_);
                QP_ = QP1(i);
            end


        end

%
%_____
_____________________________
```

BOUNDARY CONDITIONS AT UPPER RESERVOIR. PIPE 1.

```
            % Calculating Reynolds number for pipe 1 at i = 1:
            Re1(1) = ((Q1(1)/A1)*D1)/visc;

            %Calculating quasi-steady fq:
            if Re1(1) < 2300
                fq1(1) = 64/Re1(1);
            else
                fq1(1) = colebr(Re1(1),K_rough1);
            end

            %Then calculating C_star:
            if Re1(1) < 2300
```

```
                C_star(1) = 0.00476;
            else
                C_star(1) = 7.41/(Re1(1)^(log(14.3/(Re1(1)^0.05))));
            end

            %Coefficient k:
            k(1) = sqrt(C_star(1))/2;
            k(1) = corrval*k(1);


            HP1(1) = HR1; % Upstream reservoir. Constant head.
            QP_ = Q1(1); % Temporary value of QP1 = QP_
            Q_residual = tol;

        while Q_residual >= tol

            J1_neg(1) = (fq1(1)*Q1(1+1)*abs(Q1(1+1))/(2*g*D1*A1^2))+((k(1)/(2*g*A1))*((QP_-
Q1(1))/dt1));
            CM = H1(1+1)-(B1*Q1(1+1))+(J1_neg(1)*dx1);

            QP1(1) = (HP1(1)-CM)/B1;

            Q_residual = abs(QP1(1)-QP_);
            QP_ = QP1(1);
        end

%
%_____________________________________________________________________________________
_____________________________
```

BOUNDARY CONDITIONS IN THE TRANSITION BETWEEN PIPE 1 AND PIPE 2:

```
            % Calculating Reynolds number at the end of pipe 1, i = NS:
            Re1(NS1) = ((Q1(NS1)/A1)*D1)/visc;

            if Re1(NS1) < 2300
                fq1(NS1) = 64/Re1(NS1);
            else
                fq1(NS1) = colebr(Re1(NS1),K_rough1);
            end

            %Then calculating C_star:
            if Re1(NS1) < 2300
                C_star(NS1) = 0.00476;
            else
                C_star(NS1) = 7.41/(Re1(NS1)^(log(14.3/(Re1(NS1)^0.05))));
            end

            %Coefficient k:
            k(NS1) = sqrt(C_star(NS1))/2;
            k(NS1) = corrval*k(NS1);


            % Calculating Reynolds number for pipe 2 at i = 1:
            Re2(1) = ((Q2(1)/A2)*D2)/visc;
```

```
            if Re2(1) < 2300
                fq2(1) = 64/Re2(1);
            else
                fq2(1) = colebr(Re2(1),K_rough2);
            end


            %Then calculating C_star:
            if Re2(1) < 2300
                C_star2(1) = 0.00476;
            else
                C_star2(1) = 7.41/(Re2(1)^(log(14.3/(Re2(1)^0.05))));
            end

            %Coefficient k:
            k2(1) = sqrt(C_star2(1))/2;
            k2(1) = corrval*k2(1);

            QP_ = Q1(NS1); % Temporary value of QP1 and QP2
            Q_residual = tol;

        while Q_residual >= tol

            % Pipe 1:
            J1_pos(NS1) = (fq1(NS1)*Q1(NS1-1)*abs(Q1(NS1-
1))/(2*g*D1*A1^2))+((k(NS1)/(2*g*A1))*((QP_-Q1(NS1))/dt1));

            % Pipe 2:
            J2_neg(1) = (fq2(1)*Q2(1+1)*abs(Q2(1+1))/(2*g*D2*A2^2))+((k2(1)/(2*g*A2))*((QP_-
Q2(1))/dt2));

            % Pipe 1:
            CP_1 = H1(NS1-1)+(B1*Q1(NS1-1))-(J1_pos(NS1)*dx1);

            % Pipe 2:
            CM_2 = H2(1+1)-(B2*Q2(1+1))+(J2_neg(1)*dx2);


            QP1(NS1) = ((CP_1-CM_2)/(B1+B2));
            HP1(NS1) = CP_1-(B1*QP1(NS1));

            QP2(1) = QP1(NS1);
            HP2(1) = CM_2+(B2*QP2(1));

            Q_residual = abs(QP1(NS1)-QP_);
            QP_ = QP1(NS1);

        end

%_____________________________________________________________
```

BOUNDARY CONDITIONS FOR NODE 2 to N. PIPE 2.

```
        for i = 2:N2;

            %Calculating Reynolds number:
```

```
            Re2(i) = ((Q2(i)/A2)*D2)/visc;

            %Calculating quasi-steady fq:
            if Re2(i) == 0
                fq2(i)= 0;
            elseif 0 < Re2(i) < 2300
                fq2(i) = 64/Re2(i);
            else
                fq2(i) = colebr(Re2(i),K_rough2);
            end

            %Then calculating C_star:
            if Re2(i) < 2300
                C_star2(i) = 0.00476;
            else
                C_star2(i) = 7.41/(Re2(i)^(log(14.3/(Re2(i)^0.05))));
            end

            % Brunone friction coefficient:
            k2(i) = sqrt(C_star2(i))/2;
            k2(i) = corrval*k2(i);

            QP2_ = Q2(i); % Temporary value of QP2 = QP2_;
            Q2_residual = tol;

            while Q2_residual >=tol

                J2_pos(i) = (fq2(i)*Q2(i-1)*abs(Q2(i-
1))/(2*g*D2*A2^2))+((k2(i)/(2*g*A2))*((QP2_-Q2(i))/dt2));
                J2_neg(i) =
(fq2(i)*Q2(i+1)*abs(Q2(i+1))/(2*g*D2*A2^2))+((k2(i)/(2*g*A2))*((QP2_-Q2(i))/dt2));

                CP = H2(i-1)+(B2*Q2(i-1))-(J2_pos(i)*dx2);
                CM = H2(i+1)-(B2*Q2(i+1))+(J2_neg(i)*dx2);

                HP2(i) = 0.5*(CP+CM);
                QP2(i) = (CP-HP2(i))/B2;

                Q2_residual = abs(QP2(i)-QP2_);
                QP2_ = QP2(i);
            end


        end


%
%_____
_____________________________
```

BOUNDARY CONDITIONS AT PIPE END. PIPE 2.

```
            % Calculating Reynolds number at pipe end:
            Re2(NS2) = ((Q2(NS2)/A2)*D2)/visc; % Endre Q(1)

            %C alculating quasi-steady fq:
            if Re2(NS2) == 0
```

```
                fq2(NS2) = 0;

            elseif 0 < Re2(NS2) < 2300
                fq2(NS2) = 64/Re2(NS2);

            else
                fq2(NS2) = colebr(Re2(NS2),K_rough2);
            end


            %Then calculating C_star:
            if Re2(NS2) < 2300
                C_star2(NS2) = 0.00476;
            else
                C_star2(NS2) = 7.41/(Re2(NS2)^(log(14.3/(Re2(NS2)^0.05))));
            end

            %Coefficient k:
            k2(NS2) = sqrt(C_star2(NS2))/2;
            k2(NS2) = corrval*k2(NS2);

            % TIME STEP:
            t_vec(count) = t;
            t = t+dt1;

    % CP at pipe end:
    QP2_(NS2) = Q2(NS2); % Temporary value of QP2 = QP2_
    Q2_residual = tol;

    while Q2_residual >= tol

        J2_pos(NS2) = (fq2(NS2)*Q2(NS2-1)*abs(Q2(NS2-
1))/(2*g*D2*A2^2))+((k2(NS2)/(2*g*A2))*((QP2_(NS2)-Q2(NS2))/dt2));
        CP = H2(NS2-1)+(B2*Q2(NS2-1))-(J2_pos(NS2)*dx2);


        if t<tc % While valve is still closing
            tt(count) = t;

            VO_c(count) = VOI*(1-(t/tc)); %Change in valve opening, array.
            VO = VOI*(1-(t/tc)); %Change in valve opening.

            Cc_c(count) = linint(VO); % Loss coefficients, array.
            Cc = linint(VO); % Sending valve position to function "linint". Reciving flow
coefficient.

            Kv(count) = (1/Cc^2)-1; % Valve loss coefficient, f(valve opening, type)

            C3 = Kv(count)/(2*g*A2^2);
            CC3 = B2/C3;
            CC4 = (HR2-CP)/C3;

            QP2(count) = 0.5*(-CC3+sqrt((CC3^2)-(4*CC4)));
            QP2(NS2) = 0.5*(-CC3+sqrt((CC3^2)-(4*CC4)));
            HP2(NS2) = CP-(B2*QP2(NS2));


        else  % Valve is closed
```

```
            QP2(NS2) = 0;
            HP2(NS2) = CP;

        end

            Q2_residual = abs(QP2(NS2)-QP2_(NS2));
            QP2_(NS2) = QP2(NS2);

    end

    CP_c(count) = CP;

    Q1_temp(count,:) = Q1; % Pipe flow for pipe 1. Contains the flow at each node.
    H1_temp(count,:) = H1; % Head in pipe 1. Contains head at each node.
    Q2_temp(count,:) = Q2; % Pipe flow for pipe 2. Contains the flow at each node.
    H2_temp(count,:) = H2; % Head in pipe 2. Contains head at each node.



% % ____________________________________________________________________________
% % REINITIALIZE VALUES:

        for i = 1:NS1
            Q1(i) = QP1(i);
            H1(i) = HP1(i);
        end

        for i = 1:NS2
            Q2(i) = QP2(i);
            H2(i) = HP2(i);
        end

        count = count + 1;

end
```

_____ END OF SIMULATION _____

```
%%_____________________________________________________________________________
```

_____RELATIVE ANALYSIS:_____

```
tlim = length(H2_temp); % Number of time steps

% Differential pressure of the last node on pipe 2:
P_temp = (H2_temp(:,NS2)*g*rho)-3.9198e+04;
plot(t_vec,P_temp)
ylabel('dP [Pa]')
xlabel('t [s]')

% Calculation of the geometrical constant:
k1 = 1/(((L1/A1)+(L2/A2))*1000);

PL_abs = -P_temp(2);% Initial pressure loss
k2_abs = PL_abs/power(QI,2); % Initial constant k2
```

```
% Finding linear losses:
loss = [];

for i = 1:1
    loss(i,1) = -PL_abs;
end

x = 0;
for i = 2:1508
    loss(i,1)=((PL_abs/(1508-2))*x)-PL_abs;
    x = x+1;
end

for i = 1509:tlim
    loss(i,1) = 0;
end

% Relative PT with linear losses:
Q_rel_temp = k1*cumtrapz(t_vec,P_temp(:,1)-loss);
Q_1r_temp = k1*trapz(t_vec,P_temp(:,1)-loss);

Q_ct = Q_1r_temp;
Q_1 = Q_ct;
i = 1;
Q_residual = Q_ct;

% Implementing relative PT procedure:
while Q_residual > tol

    Q_ct = k1*cumtrapz(t_vec,P_temp-((PL_abs/(Q_1*abs(Q_1))).*(Q_ct-Q_1).*abs(Q_ct-Q_1)));
    Q_lossterm_q = ((PL_abs/(Q_1*abs(Q_1))).*(Q_ct-Q_1).*abs(Q_ct-Q_1));
    Q_(i) = k1*trapz(t_vec,P_temp-((PL_abs/(Q_1*abs(Q_1))).*(Q_ct-Q_1).*abs(Q_ct-Q_1)));
    Q_residual = abs(Q_(i)-Q_1);
    Q_1 = Q_(i);
    i = i+1;
end

% Relative losses:
for i = 1:length(Q_ct)
    relativeloss(i) = ((PL_abs/(Q_1*abs(Q_1))).*(Q_ct(i)).*abs(Q_ct(i)));
end

% Comparing relative flow and actual flow:
figure(1)
plot(t_vec,Q2_temp(:,NS2)); % Actual flow
hold on
plot(t_vec,Q_ct); % Actual flow
hold off
```

Published with MATLAB® R2015a